EUROPEAN COMMISSION
5th EURATOM FRAMEWORK PROGRAMME 1998-2002
KEY ACTION : NUCLEAR FISSION

HTR-M

European Project for the development of HTR Technology - Materials for the HTR

CONTRACT N°
FIKI-CT-2000-00032
&
FIKI-CT-2001-00135

STATE OF THE ART REVIEW OF GRAPHITE

MATERIALS AND BEHAVIOUR

by

M W Davies, NNC

G Haag, FZJ

Dissemination level : CO
Document Number: HTR-M-02/06-D-3.1.37
Deliverable 3.1

State of the art review of graphite

materials and behaviour

by

M W Davies (NNC)
and G Haag (FZJ)

C6463/TR/011
Issue 02
August 2004

DOCUMENT ISSUE RECORD
(engineering documents)

Adding value through knowledge

Document Title :	State of the art review of graphite materials and behaviour.
Project Reference:	C6463

Purpose of Issue : For use

Security Class : Commercial-in-Confidence

Issue	Description of Amendment	Originator/ Author	Checker	Approver	Date
01	First issue				
		M W Davies G Haag	D E Buckthorpe	T Lennox	
02	Final Issue including comments from HTR-M partners	M W Davies	D E Buckthorpe	T Lennox	August 2004

Total number of pages:	Intro:	(i)-(v)	Text	1 - 5	Tables	T1 - T4	Figures	F1	Appendices	A1-A6 B1-B25

Previous issues of this document shall be destroyed or marked **SUPERSEDED**

Distribution: S. Casalta (EC), Mr D E Buckthorpe, SINTER, EDMS

3050aJan01 Controlling procedure - QP11, QP40 *Docprodref*

Table of Contents

List of Tables

List of Figures

Summary

Graphite has been used as a neutron moderator in a variety of different reactors. These include the Magnox Reactors, Advanced Gas-cooled Reactors (AGRs), High Temperature Reactors (HTRs), RBMKs, Research Reactors and Materials Testing Reactors (MTRs). The amount of nuclear grade graphite currently manufactured worldwide is relatively small. However, there has recently been a renewal of interest in HTRs in the world. The European Commission is supporting a number of projects for the development of HTR technology, with a view to creating the technological basis for the industrial emergence of HTRs in Europe by 2010.

The properties of graphite in a reactor environment have been extensively studied since the early 1940s and a good understanding of the significant and complex property changes which take place in the material has been gained. Most of the available data have been obtained by irradiating small graphite samples in MTRs. Unfortunately, almost all the graphites previously irradiated are no longer available. In addition, most of the irradiation temperatures investigated will have been $<550^{o}$C, whereas for HTRs the graphite temperatures will be $>550^{o}$C. The behaviour of currently available graphites will therefore have to be determined by experiments in a MTR over the appropriate irradiation dose and temperature range.

A review of the current situation regarding graphite has been carried out for the European HTR project. Part of this work has been undertaken under HTR-M and involved carrying out a review of available data on the irradiation behaviour of different graphites at high temperatures. This work is the subject of this report.

In the past, only a small number of irradiation programmes were aimed at determining the irradiation behaviour of graphites at high temperatures, i.e. $>600^{o}$C. Two of the most significant in the past were for the European Dragon HTR programme, and the German HTR programme. Unfortunately most of the data obtained by other countries are confidential and cannot therefore be published in open literature. However, the data from the German HTR programme are available for publication and those concerning the graphite grade ATR-2E (manufactured by SGL Carbon Company) have been included in this report.

1 Introduction

Graphite has been used as a neutron moderator in a variety of different reactors. These include the Advanced Gas-cooled Reactors (AGRs), Magnox Reactors, High Temperature Reactors (HTRs), RBMKs, Research Reactors and Materials Testing Reactors (MTRs). The amount of nuclear grade graphite currently manufactured worldwide is relatively small, and broadly consists of graphite for AGR fuel sleeves and prototype HTRs (one in Japan and one in China). However, there has recently been a renewal of interest in HTRs in the world. The design of the Pebble Bed Modular Reactor (PBMR), led by ESKOM (South Africa), and the Gas-Turbine Modular Helium Reactor (GT-MHR) led by an international consortium (Russia, USA, France and Japan) are at an advanced stage. The European Commission is also supporting a number of projects for the development of HTR technology, with a view to creating the technological basis for the industrial emergence of HTRs in Europe by 2010.

The behaviour of graphite in a reactor environment has been extensively studied since the early 1940s and a good understanding of the significant and complex property changes which take place in the material has been gained. Most of the available data have been obtained by irradiating small graphite samples in MTRs. Unfortunately, almost all the graphites previously irradiated are no longer available. In addition, most of the irradiation temperatures investigated will have been $<550^{o}C$, whereas for HTRs the graphite temperatures will be $>550^{o}C$. The behaviour of currently available graphites will therefore have to be determined by experiments in a MTR over the appropriate irradiation dose and temperature range.

It was considered necessary to first of all carry out a review of the current situation regarding graphite for the European HTR project. Part of this work has been undertaken under HTR-M, and involved carrying out a review of available data on the irradiation behaviour of different graphites at high temperatures. This work is the subject of this report (additional work is being carried out under HTR-M1 and involves the irradiation of a selection of currently available graphites in the High Flux Reactor at Petten, details of this work will be covered in a separate report, in addition there is a need to develop an appropriate database for assembling the existing and future graphite data, this is also covered in a separate report, Ref. 1).

2 Nuclear graphite manufacture

Natural graphite is not plentiful and so there is a need to manufacture ‘artificial’ graphites for large scale applications, such as electric arc furnaces and nuclear reactor cores. Modern graphite manufacture starts with a high molecular weight hydrocarbon - often a natural pitch or a residue of crude oil distillation - which is first converted to coke by heating in the absence of air. This process is long and complex, both in the choice of initial stock and its subsequent thermal treatment, and can take weeks to perform. During the process, the carbon atoms form a ‘mesophase’, where they order themselves in extensive hexagonal clumps.

The coke is then calcined, crushed and screened to get a specific distribution of particle sizes - typically 1 mm or less. Next, the particles are mixed with a binder pitch (generally coal tar pitch) in heated mixers to obtain a plastic paste at a uniform

temperature. The paste is then charged into an extrusion press or into a mould to form rough blocks nearly of the shape eventually required.

One crucial property is now already determined. This is the anisotropy of the graphite, which is so vital in determining it's behaviour under irradiation (see Section 3). The crystal lattice in graphite can at best only be continuous over the coke particle dimensions - so if these particles are randomly oriented the aggregate will be macroscopically isotropic, despite the inherent microscopic anisotropy of the graphite's atomic lattice. However, coke particles are seldom spherically symmetric, and the directional forces used in moulding or extruding tend to align them in preferred directions, leading to anisotropy on the 'block' scale. For example, extrusion tends to align crystallite basal planes parallel to the extrusion direction, whereas pressing in a mould tends to align them perpendicular to the pressing direction.

The 'green' pieces from the forming stage are then baked in a furnace, at a temperature of at least 800^{o}C, for several weeks. After baking, the pieces are allowed to cool very slowly. The baking process changes the binder pitch into amorphous carbon. As the volatiles are released, an extensive pore network is created. As a result, the apparent density of the graphite is quite low, and so the baked article is generally impregnated with a suitable impregnant (pitch), and then re-baked (like baking, re-baking changes the impregnant pitch into carbon, but now the process is much faster). This procedure is repeated until the required density is reached. This may involve one, two or three impregnation/baking cycles. As well as increasing the density, there is also a general improvement in mechanical properties, and a decrease in porosity and hence permeability.

Finally, the amorphous carbon material is transformed into crystalline graphite, at a temperature between 2800^{o}C and 3300^{o}C, in a graphitising furnace. The blocks are stacked in close proximity in the furnace and covered completely with carbon particles as a thermal insulation. A large current is passed through the bed to raise the temperature of the blocks and maintain it at the required level. After graphitisation, the pieces are allowed to cool very slowly.

For nuclear applications, the graphite has to be as free as possible from impurities. Most of the impurities present will become activated during the operating life of the reactor, which will give rise to operational problems, as well as decommissioning and final disposal problems. Most impurities, however, are volatile and so disappear during graphitisation. To remove as much of the remainder as possible, halogens are added generally during graphitisation to aid the conversion of metal impurities and boron particularly, to their more volatile halides (extremely low boron levels are important from a reactor physics point of view as it is a very strong neutron absorber).

The graphite blocks are then machined to the dimensions of the finished product. Fortunately, graphite is generally very machinable and so tight tolerances can be achieved.

3 Irradiation behaviour of graphite

One of the main functions of the graphite is to slow down fast neutrons (which are born with an average energy of ~ 2MeV) to thermal energies of < 1eV. This is achieved by elastic collisions between the neutrons and the carbon nuclei. When a carbon atom is hit by a fast neutron, it is displaced from its lattice position and has sufficient energy to displace a large number of other carbon atoms. Each of these in turn can have sufficient energy to displace many other carbon atoms. Thus a single fast neutron/carbon nucleus impact can lead to a very large number of displaced carbon atoms. The fast neutron itself can go on to create many more displaced carbon atoms as it slows down, which in turn displace more carbon atoms as before. The displaced carbon atoms generally end up between the layer planes and can coalesce to form anything from sub-microscopic clusters of a few atoms up to large interstitial clusters containing many hundreds of atoms. The interstitial loops force the planes apart and so the crystals grow in the direction perpendicular to the planes ('c' direction). The displaced atoms will leave vacancies which can themselves combine to form large vacancy loops. This results in the crystals contracting in the direction parallel to the planes ('a' direction).

The nett effect on a polycrystal is thus growth and shrinkage. Pile Grade A (PGA) graphite, used in the UK's Magnox reactors, was manufactured using a needle coke and the blocks were formed by extrusion. This tended to align the crystal planes in the direction of extrusion and so when irradiated the graphite exhibited growth perpendicular to the extrusion direction and shrinkage parallel to the extrusion direction. The behaviour was thus very anisotropic. Gilsocarbon graphite, however, which was used for the UK's AGRs was manufactured using spherical gilsonite coke and the blocks were moulded in a press. This resulted in an isotropic graphite which when irradiated exhibited shrinkage in both the parallel and perpendicular directions.

The dimensional change behaviour of Gilsocarbon graphite was determined in various MTRs over a temperature range of 350^{o}C to 550^{o}C (at approximately 50^{o}C intervals). These are shown in Figure 1. It can be seen that for each of the temperatures, the graphite initially shrinks, reaches a maximum shrinkage, before turning around and growing again. There was a clear difference between the behaviour of the graphite at the five temperatures, with a difference in the maximum shrinkage and the irradiation dose at which the maximum occurred. Given that graphite components used for the moderator and reflector have dose and temperature gradients within them, it was extremely important for the core designer to know the dimensional change behaviour of the graphite over the full irradiation dose expected and over the full range of temperatures.

Material properties are also affected by irradiation, the most important ones from a core design point of view being strength, Young's modulus and Coefficient of Thermal Expansion (CTE). The strength and Young's modulus of Gilsocarbon graphite are both increased by irradiation, whereas although CTE also initially increases, it subsequently falls, reducing to around half the unirradiated value over the dose range of interest (in the UK reactors, weight loss due to oxidation of the graphite by the carbon dioxide coolant is also an important issue, weight loss decreases strength and Young's modulus, but appears to have little effect on CTE.).

4 Previous irradiation programmes

There have been numerous graphite irradiation programmes carried out over the years by many different countries. These have been primarily aimed at getting all the necessary data on graphite behaviour for the particular reactor core design, whether it be Magnox, AGR, or HTR. Some of the properties of interest and the way in which they are measured are given in Appendix A.

For the UK irradiation programmes in support of Magnox and AGRs, the PGA and Gilsocarbon graphites were irradiated in PLUTO, DIDO, BEPO, DFR (all in the UK) and in BF3 (France). All such irradiations were carried out at temperatures <550^{o}C. A very large amount of data has also been generated by other countries in their irradiation programmes. The problem is that much of it is still subject to confidentiality/secrecy. However, the IAEA is currently producing a database on nuclear graphite and it is hoped that the data will eventually be stored in it, even though it might remain restricted. The database is being updated periodically as more data are added.

Of all the irradiation programmes carried out, only a small number of them were aimed at determining the irradiation behaviour of graphites at high temperatures, i.e. >600^{o}C. Two of the most significant programmes in the past were for the European Dragon HTR programme, and the German HTR programme. Data have also been obtained by the Japanese for their HTR programme.

For the Dragon HTR programme, many different graphites were irradiated in the Petten HFR and over a temperature range of 430 to 1450^{o}C and up to a dose of ~2.0x10^{22} n/cm^{2}. These included graphites which were petroleum coke based, pitch coke based, isotropic, anisotropic, fine grain, medium grain, moulded (pressed) and extruded with zero, one, two or three impregnations. For the German HTR, the selected graphites were also irradiated in the Petten HFR and over a temperature range of 300 to 1250^{o}C and again up to a dose of ~2.0x10^{22} n/cm^{2}.

5 Existing data at high temperatures

Although a significant amount of data exists on the irradiation behaviour of graphites at high temperatures, as stated above, much of it is still subject to confidentiality/secrecy and cannot therefore be published in open literature at the current time. It is hoped that the restrictions will be lifted in the future (further issues of this document can be produced as more data becomes de-restricted, and it is thought beneficial to include them. in any event, the data could be included on the SINTER database).

Fortunately, it is possible at the present time to publish the data from the German HTR programme. The data are for graphite grade ATR-2E and are presented in Appendix B as a number of graphical plots. The properties covered are dimensional change (linear and volume), Young modulus, CTE and electrical resistivity. The data are presented over a temperature range of 300-1250^{o}C. The data relating to the curves will be stored in tabular form on the SINTER database (examples of which are given in Tables 1 to 5). More data on other graphites could be made available in the future.

However, most of the data have never been published in open literature, and need to be extracted from old files before being lost.

As mentioned earlier, a programme of graphite irradiation at high temperature is being carried out under HTR-M1. As the data become available, they will also be included on the SINTER database.

6 Conclusions

Graphite has been used as a neutron moderator in a variety of different reactors, and there has recently been a renewal of interest in HTRs in the world. In particular the European Commission is supporting a number of projects for the development of HTR technology, with a view to creating the technological basis for the industrial emergence of HTRs in Europe by 2010.

Most of the available data on the irradiation behaviour of graphite have been obtained by irradiating small samples in MTRs. Unfortunately, almost all the graphites previously irradiated are no longer available. Before embarking on the planned irradiation programme for the European HTR project it was first of all necessary to carry out a review of the situation regarding graphite data.

It was found that only a small number of irradiation programmes carries out in the past were aimed at determining the irradiation behaviour of graphites at the high operating temperatures associated with a HTR, i.e. >600^{o}C. Two of the most significant in the past were for the European Dragon HTR programme, and the German HTR programme. Unfortunately most of the data obtained by other countries are confidential and so far are not published in open literature. However, data from the German HTR programme are available for publication and some have been included in this report.

7 References

Ref	Title
1	M W Davies. Report on database of graphite properties suitable for use by designers. HTR-M-02/6-D-3.1.38. NNC Report C6463/TR/012

Table 1 Relative linear dimensional change (%) at 600°C for grade ATR-2E

Fast Neutron Fluence (10^{21}/cm^2(EDN))	Rel. Length Change (%) 595-605°C par.
3,21	-0,77
9,31	-2,49
12,41	-2,98
17,59	-2,00
4,29	-1,03
7,79	-2,11
10,99	-2,98
16,49	-2,78
4,57	-1,03
9,57	-2,66
13,12	-3,00
18,94	-1,64
4,70	-1,08
9,40	-2,52
12,90	-3,10
18,73	-2,00
3,90	-0,92
4,51	-1,08
8,41	-2,67
11,61	-3,06
3,80	-0,82
6,30	-2,10
8,75	-2,78
12,95	-2,94
2,42	-0,55
8,12	-2,09
10,77	-2,77
15,32	-2,71

Fast Neutron Fluence (10^{21}/cm^2(EDN))	Rel. Length Change (%) 595-605°C perp.
2,80	-0,51
8,80	-1,53
11,65	-1,66
16,52	-0,32
4,48	-0,83
8,48	-1,69
11,83	-1,41
17,53	1,12
4,40	-0,82
9,80	-1,90
13,20	-1,74
18,90	0,19
4,64	-0,87
9,74	-2,05
13,34	-1,86
19,04	0,67
3,56	-0,71
8,86	-1,85
11,26	-2,05
15,41	-1,23
4,67	-0,89
8,97	-1,87
12,27	-1,83
4,06	-0,81
7,06	-1,70
9,71	-2,07
14,31	-1,42

Table 2 Relative Young's modulus change (E/Eo) at 600°C for grade ATR-2E

Fast Neutron Fluence (10^{21}/cm^2(EDN))	Young's Modulus Change E/E_0 at 600°C
3,21	1,81
9,31	2,19
12,41	2,08
4,29	1,97
7,79	2,21
10,99	2,13
4,57	1,96
9,57	2,70
13,12	2,09
4,70	1,97
9,40	2,45
12,90	2,52
3,90	1,91
4,51	1,95
8,41	2,58
11,61	2,14
3,80	1,92
6,30	2,19
8,75	2,02
12,95	1,94
2,42	1,87
8,12	2,22

Fast Neutron Fluence (10^{21}/cm^2(EDN))	Young's Modulus Change E/E_0 at 600°C
10,77	2,25
15,32	2,08
2,80	1,83
8,80	2,28
11,65	2,27
4,48	1,99
8,48	2,63
11,83	2,70
4,40	1,95
9,80	2,63
13,20	2,30
4,64	1,96
9,74	2,74
13,34	2,57
3,56	1,95
8,86	2,49
11,26	2,38
4,67	1,99
8,97	2,56
4,06	1,97
7,06	2,23
9,71	2,25

Table 3 Relative CTE change at 600°C for grade ATR-2E

Fast Neutron Fluence (10^{21}/cm^2(EDN))	Rel. Therm. Exp. Change (%) at 600°C
3,21	16,7
9,31	-10,0
12,41	-26,8
17,59	-33,3
4,29	14,0
7,79	-0,7
10,99	-25,1
16,49	-33,4
4,57	9,7
9,57	-22,0
13,12	-38,6
18,94	-42,3

Fast Neutron Fluence (10^{21}/cm^2(EDN))	Rel. Therm. Exp. Change (%) at 600°C
2,80	17,8
8,80	-1,6
11,65	-23,2
16,52	-35,6
4,48	19,2
8,48	-15,4
11,83	-29,3
17,53	-41,8
4,40	17,0
9,80	-19,0
13,20	-32,3
18,90	-35,8

Table 4 Relative electrical resistivity change (%) at 600°C for grade ATR-2E

Fast Neutron Fluence (10^{21}/cm^2(EDN))	Electr. Resist. Change ρ/ρ_0 par. at 600°C
3,21	3,19
9,31	3,15
12,41	3,54
17,59	3,48
4,29	3,25
7,79	3,21
10,99	3,11
16,49	3,45
4,57	3,23
9,57	3,15
13,12	3,18
18,94	3,79
4,70	3,16
9,40	3,12
12,90	2,95
18,73	3,72
3,90	3,20
4,51	3,29
8,41	3,20
11,61	3,16
3,80	3,37
6,30	3,32
8,75	3,17
12,95	3,34
2,42	3,24
8,12	3,21
10,77	3,18
15,32	3,29

Fast Neutron Fluence (10^{21}/cm^2(EDN))	Electr. Resist. Change ρ/ρ_0 perp. at 600°C
2,80	3,39
8,80	3,12
11,65	3,04
16,52	3,14
4,48	3,17
8,48	3,06
11,83	2,95
17,53	3,61
4,40	3,14
9,80	3,05
13,20	2,96
18,90	3,70
4,64	3,22
9,74	3,09
13,34	3,00
19,04	3,78
3,56	3,18
8,86	3,05
11,26	2,98
15,41	3,21
4,67	3,17
8,97	3,02
12,27	2,94
4,06	3,18
7,06	3,15
9,71	3,10
14,31	3,19

Table 5 Relative volume change (%) at 600°C for grade ATR-2E

Fast Neutron Fluence (10^{21}/cm^2(EDN))	Rel. Volume Change at 600°C
3,21	3,19
9,31	3,15
12,41	3,54
17,59	3,48
4,29	3,25
7,79	3,21
10,99	3,11
16,49	3,45
4,57	3,23
9,57	3,15
13,12	3,18
18,94	3,79
4,70	3,16
9,40	3,12
12,90	2,95
18,73	3,72
3,90	3,20
4,51	3,29
8,41	3,20
11,61	3,16
3,80	3,37
6,30	3,32
8,75	3,17
12,95	3,34
2,42	3,24
8,12	3,21
10,77	3,18
15,32	3,29

Fast Neutron Fluence (10^{21}/cm^2(EDN))	Rel. Volume Change at 600°C
2,80	3,39
8,80	3,12
11,65	3,04
16,52	3,14
4,48	3,17
8,48	3,06
11,83	2,95
17,53	3,61
4,40	3,14
9,80	3,05
13,20	2,96
18,90	3,70
4,64	3,22
9,74	3,09
13,34	3,00
19,04	3,78
3,56	3,18
8,86	3,05
11,26	2,98
15,41	3,21
4,67	3,17
8,97	3,02
12,27	2,94
4,06	3,18
7,06	3,15
9,71	3,10
14,31	3,19

Figure 1 Dimensional change behaviour of Gilsocarbon graphite

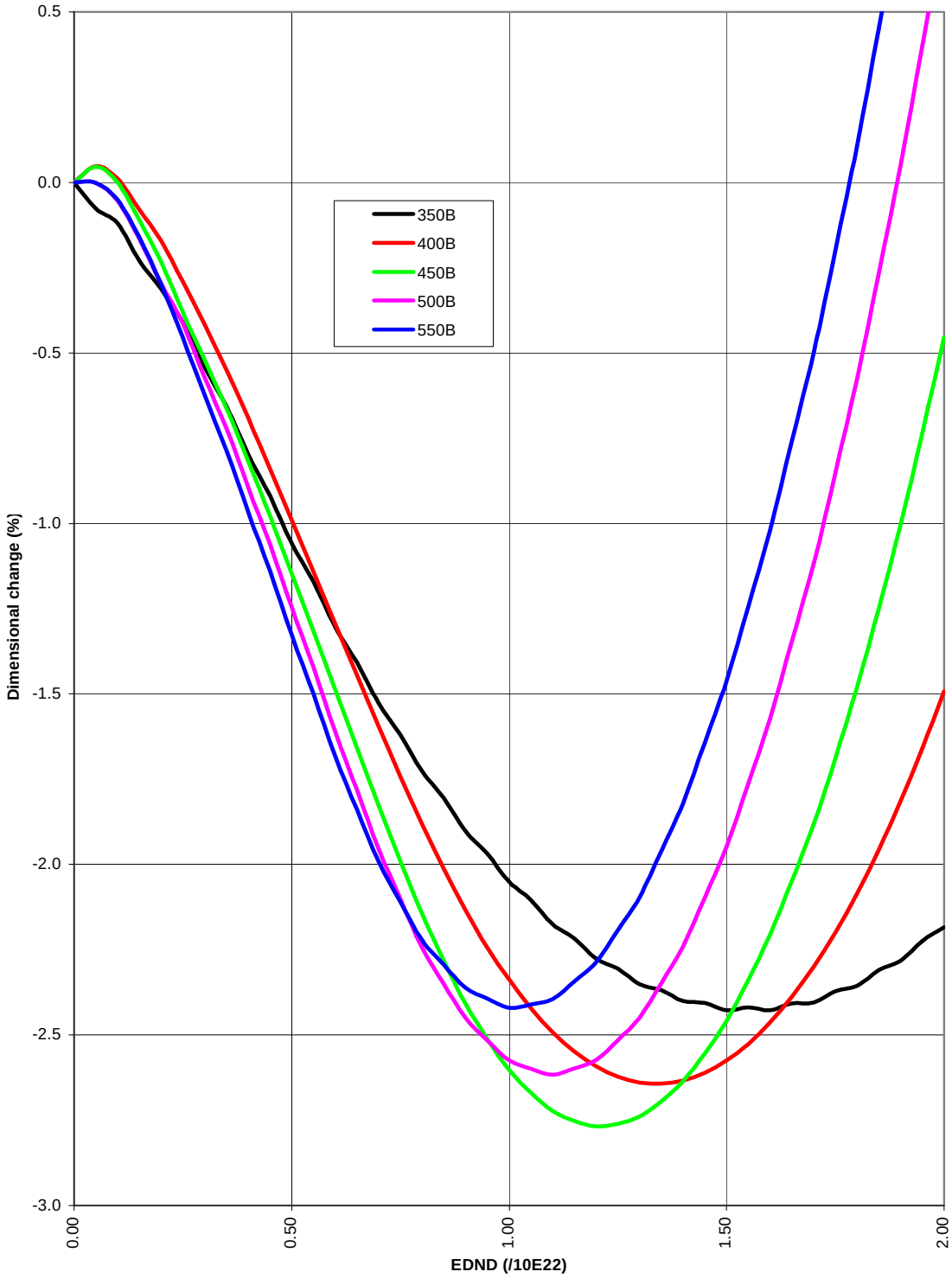

Appendix A - Material property measurements

1 Introduction

In a HTR graphitic structural components are subjected to various temperature and neutron flux conditions. Physical properties of graphite such as dimensions, Young's modulus, thermal expansivity, thermal conductivity, and strength change under fast neutron irradiation, and in most cases these property changes are strongly temperature dependent. In addition, graphitic components are exposed to mechanical loads and temperature gradients. All these influences lead to internal stresses which can destroy structural components.

As a contribution to the database needed for the design of the graphite structures, former KFA Jülich has sponsored a programme of graphite irradiation experiments in HFR at Petten (Ref. A.1 and A.2) over more than 20 years.

The Petten HFR is a high power materials testing reactor. It is of the tank-in-pool type, it is light-water cooled and moderated, and since 1970 it is operated at 45 MW at a prescribed schedule of 11 cycles per year, each comprising 25 operation days and 3 shut-down days. Before 1970, the reactor power was only 30 MW. The reactor provides a variety of irradiation possibilities in the reactor core, the reflector region as well as outside the reactor vessel in so-called poolside facilities.

A huge campaign for the development and qualification programme of a graphite to provide a design base to the German HTR Programme was launched at the beginning of 1970s. After approximately 20 years, the irradiation programme was finished. The irradiation capsules contained unstressed samples or creep specimens under tensile or compressive stress. Samples have been irradiated in up to six fluence steps, with intermediate measurements of their properties.

The objective of the so-called *basic properties* graphite irradiation experiments using unstressed specimens has been the testing of reflector and matrix graphites covering the fluence dependence of all relevant material properties such as linear dimensions, density, porosity, Young's modulus, thermal expansion coefficient, thermal conductivity, and electrical resistivity.

The samples, generally 6 mm ∅ x 25 mm are held in drums which are suspended in multi-channel reloadable irradiation thimbles having a useful internal diameter of 30 mm. The drums are instrumented with thermocouples and are fitted with neutron fluence monitors which are analysed for each irradiation step. Sample temperature is controlled by the usual technique of gas gaps and variable inert gas mixtures (He and Ne).

Irradiation creep which relieves stresses, is another important parameter in the design of HTRs, where relevant stresses can be generated due to thermal and neutron flux loads. Special devices have been designed and employed at HFR, allowing irradiation under stress of various grades of graphite up to very high fluences ($1x10^{26}$ m^{-2} EDND) and in a wide temperature range (570 to 1170 ^{o}C). Creep measurements have taken place out-of-pile at intervals of irradiation.

The experimental procedure is to irradiate samples for a specified fluence interval, then to dismantle the rigs, recover the samples and to measure the properties. Samples are reloaded in new rigs and re-irradiated for the next step.

2 Graphite Grade ATR-2E

This graphite irradiation data review is concentrated on the German nuclear graphite ATR-2E which has been tested in great detail under fast neutron irradiation. This material is no longer available, but for future high temperature gas-cooled nuclear reactors similar graphites will be used since ATR-2E graphite was manufactured according to conventional production techniques.

ATR-2E Graphite was developed and manufactured by the SIGRI Elektrographit GmbH company since the beginning of the 1970s to replace Gilsonite coke as a raw material for isotropic nuclear graphite. ATR-2E was manufactured from an isotropic special pitch coke using coal tar pitch as the binder. Bodies of 400 mm in diam. and up to 1000 mm long were formed by extrusion and the final properties which can be seen in Table 1 were achieved by a double impregnation again using coal tar pitch. Maximum particle size was about 1 mm, and the ash content approximately 400 ppm.

Besides the good properties of the final product the choice of a German pitch coke (from VfT company, Essen, Germany) as a domestic raw material was a consequence of the 1973/74 oil crisis.

For comparing physical property data it is very important to know according to which method (standard method, if possible) the data were measured. Therefore, some of the methods used in the German irradiation programme are shortly described.

3 Property measurements

3.1 **Determination of CTE** (according to DIN 51909)

The *linear thermal expansion coefficient* describing the length of a body as a function of temperature is defined as

$$\alpha(\vartheta) = \frac{1}{l} \cdot \frac{dl}{d\vartheta}$$

where,

l is the length of the test specimen at temperature ϑ;

$\frac{dl}{d\vartheta}$ is the length change with temperature.

The *average linear thermal expansion coefficient* $\alpha(\vartheta_1, \vartheta_2)$ is the average for a particular temperature interval $(\vartheta_1, \vartheta_2)$, where

$$\alpha(\vartheta_1, \vartheta_2) = \frac{1}{l_1} \cdot \frac{l_2 - l_1}{\vartheta_2 - \vartheta_1} = \frac{1}{l_1} \cdot \frac{\Delta l}{\Delta \vartheta}. \quad (1)$$

The average linear thermal expansion coefficient is determined by means of a push-rod dilatometer. The prismatic test specimen is contained in a sample holder made from low expansivity material (such as flint glass). It is heated in a furnace and the length change is transmitted by a push-rod to a mechanical, optical, or electronic measuring system outside the furnace. The average linear thermal expansion coefficient is calculated from the measured length change, the original length, and the temperature change of the test specimen according to equation (1), taking the expansion of the sample holder and the push-rod into account.

The furnace is capable of holding the temperature constant to within ±0.5% over the length of the test specimen. The temperature measuring device, for example, a thermocouple with indicating instrument, is accurate to within ±0.5%, to determine the average test specimen temperature. The mechanical, optical or electronic length measurement device (error limits ±0.05 μm) is suitable for temperatures above 300°C in vacuum or in a protective gas atmosphere. The instrument for measuring the length of a specimen has an error limit of ±0.2%.

The test specimens are machined on all surfaces by turning or grinding. Particular attention was paid to ensure the specimen end surfaces are plane and parallel.

3.2 **Determination of Electrical Resistivity** (according to DIN 51911)

The electrical resistivity, ρ, of a specimen with constant cross section A is defined by the following equation.

$$\rho = \frac{U}{I} \cdot \frac{A}{l} \qquad (2)$$

where,

U is the voltage drop between the potential contacts;
I is the current through the test specimen;
l is the distance between the potential contacts.

A constant direct current is passed through the specimen. The electrical resistivity is calculated according to equation (2).

A DC source (ripple of $\leq 0.5\%$) is used, with adjustable current intensity and sufficient power to make sure that current intensity and voltage are accurate to within ±0.5%. The current intensity measuring device is accurate to within ±0.5%, too. The electrical current is supplied to the front surfaces of the specimen such that at the potential contacts a homogeneous current distribution is guaranteed. Point electrodes are put on the centre of the front surfaces of the specimen. The distance between the potential contacts must be at least two times the largest width of the specimen. The radius of curvature of the potential contacts (points or knife edges) is ≤ 0.25 mm. The uncertainty of the distance between the potential contacts as well as the transverse dimensions of the specimen are determined with a maximum uncertainty of ±0.5%.
Specimens of circular cross section with the front surfaces perpendicular to the longitudinal axis are used. The length is approximately five times the largest transverse dimension of the specimens. The specimens were air-dried.

On each side face of the specimen with rectangular cross-sections, four measurements were performed turning the specimen end for end and reversing the current direction. After each set of four measurements the specimen is rotated by 90°. The measuring current so small that the resistance of a specimen does not change more than ±0.5% by temperature increase during the measuring time. For most graphitic materials an excessive temperature increase can be avoided applying current densities smaller than 1 A/cm^2.

3.3 Determination of Young's Modulus (according to DIN 51915)

The Young's Modulus, E, of a body is defined as the ratio of the stress, σ, and the resulting strain, ε. E can be determined as static modulus of elasticity under static load or dynamically from sound velocity v_s. according to equation (3),

$$E_{dyn} = v_s^2 \cdot \rho_R \quad (3)$$

where ρ_R is the apparent density of the test specimen.

The stress/strain correlation is non-linear in the case of carbon and graphite materials. The static E modulus resulting from the line connecting zero-point and actual stress-strain value (the so-called secant modulus) is always smaller than the dynamic Young's modulus resulting from the tangent of the stress-strain curve at zero-point.

The Young's modulus data given in this report were measured according to the so-called resonance method. In a prismatic specimen with constant cross-section and length l, longitudinal oscillations are induced. The frequency is varied until the test specimen oscillates at maximum amplitude yielding the frequency f_0 of the basic oscillation. The sound velocity v_s is calculated from equation (4),

$$v_s = 2 \cdot l \cdot f_0 \quad (4)$$

yielding the Young's modulus according to equation (5)

$$E_{dyn} = 4 \cdot l^2 \cdot f_0^2 \cdot \rho_R \,. \quad (5)$$

Prismatic test specimens with constant circular cross-section are used. The end planes are perpendicular to the longitudinal axis. The requirement that the length of the test specimen has to be more than three times the largest transverse dimension is fulfilled.

3.4 Determination of Bulk Density (according to DIN 51918)

The bulk density, ρ_R, of a specimen is the ratio of the mass m and the total volume V_R consisting of the volume of the solid matter as well as of all pores.

$$\rho_R = \frac{m}{V_R} \quad (8)$$

The dried specimen was weighed in air. Then, the accessible pores of the specimen were filled with water. Finally, the volume of the specimen was determined from its buoyancy in water. The weight of the test specimen was determined using a

balance with maximum error limits of 10^{-4} of the mass of the specimen; the weighing dish was replaced by a short suspension.

Test samples of any size and geometry can be used, if only the surface is sufficiently smooth to enable drying the water-impregnated sample. Loosely adherent material was removed, e.g., by brushing. The test samples were dried in a drying oven for at least two hours at (110±5)°C and then cooled to room temperature 18 to 28 °C in a desiccator with drying medium. Except when required for the weighing procedures the impregnated specimens were kept covered with water at all times.

In the case of prismatic, regularly shaped specimens one would normally determine the bulk density from the mass and the linear dimensions of the test specimen. However, the determination of this so-called geometric density requires a very perfect geometry which may no more exist after irradiation (banana-shaped specimens due to irradiation induced internal stresses; oval instead of originally circular cross-section due to graphite texture) and post-irradiation handling (broken edges). Therefore, the bulk density was measured geometrically as well as by buoyancy to detect specimens with irregular geometric changes.

Table A.1 Physical properties of ATR-2E graphite (unirradiated)

			Mean values
Bulk density	g/cm^3		1.77
Thermal Expansivity CTE (20-200°C)	$10^{-6}/K$	$\parallel$	4.2
		$\perp$	4.5
Factor of Anisotropy $CTE_{\perp}/CTE_{\parallel}$ (20-500°C)			1.07
Dynamic Young's Modulus	10^3 N/mm^2	$\parallel$	9.2
		$\perp$	8.0
Bending Strength	N/mm^2	$\parallel$	20.5
		$\perp$	16.4
Compressive Strength	N/mm^2	$\parallel$	53.5
		$\perp$	54.1
Tensile Strength	N/mm^2	$\parallel$	11.7
		$\perp$	10.0
Electrical Resistivity	$\Omega \cdot \mu m$	$\parallel$	9.5
		$\perp$	10.5
Thermal Conductivity at 30°C	$W/m \cdot K$	$\parallel$	150
		$\perp$	140
Poisson's Ratio			0.15

Appendix B - Irradiation Data on ATR-2E Graphite

1 Introduction

In this Appendix, the presently available irradiation data on ATR-2E graphite are presented in graphical form. The properties covered are dimensional change (linear and volume), Young's modulus, CTE and electrical resistivity. The temperatures range from 300-1250^{o}C. The actual data used to generate the graphs are available in a form which can be fed as Microsoft Excel templates into any database. They can be found on the SINTER database.

2 List of figures

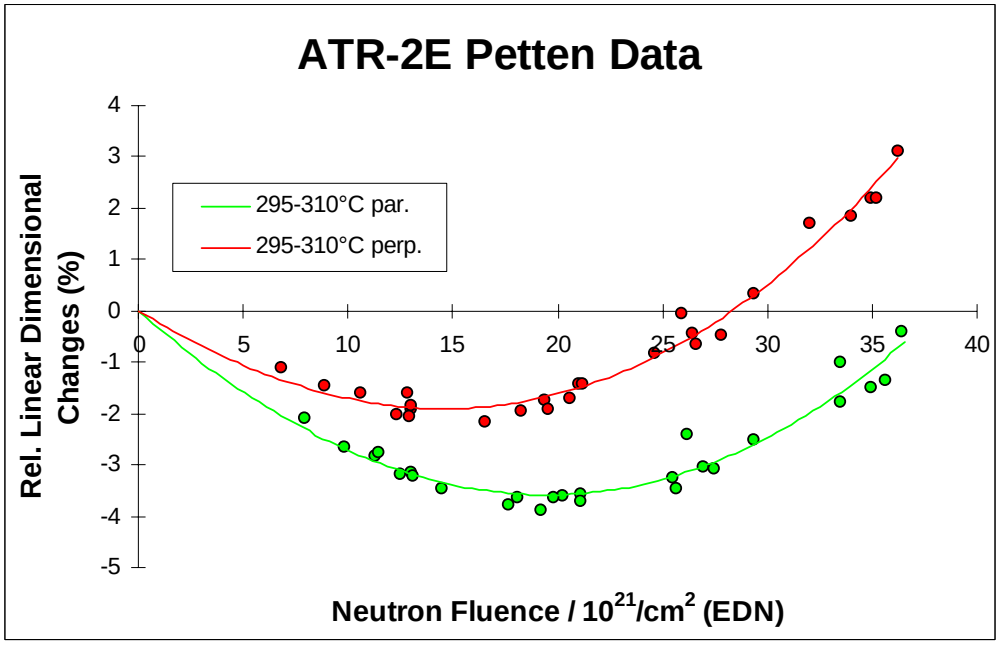

Figure B/1 Relative linear dimensional change (%) - 295-310°C

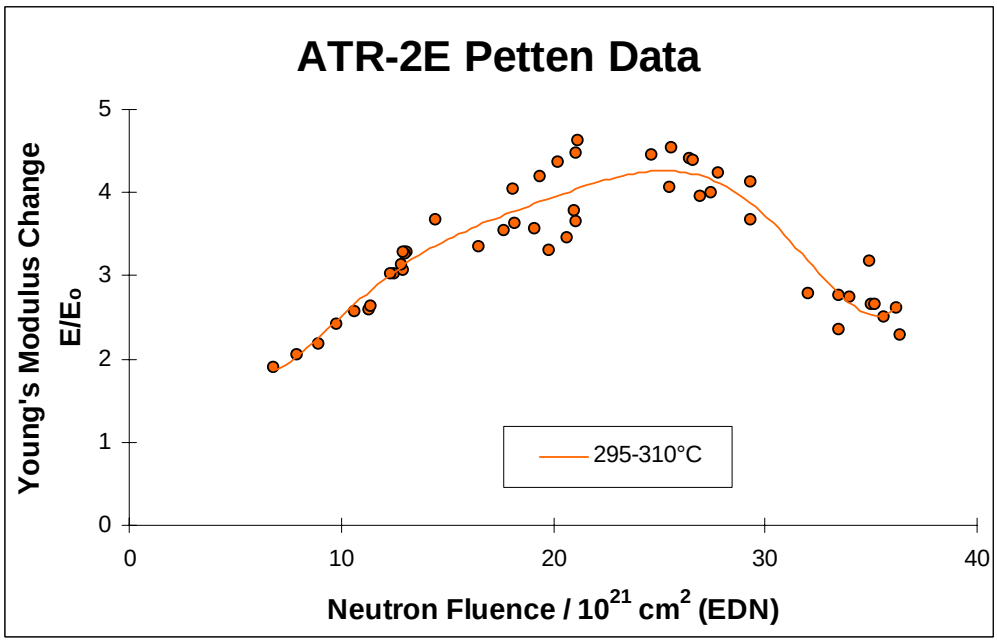

Figure B/2 Relative Young's modulus change (E/Eo) - 295-310°C

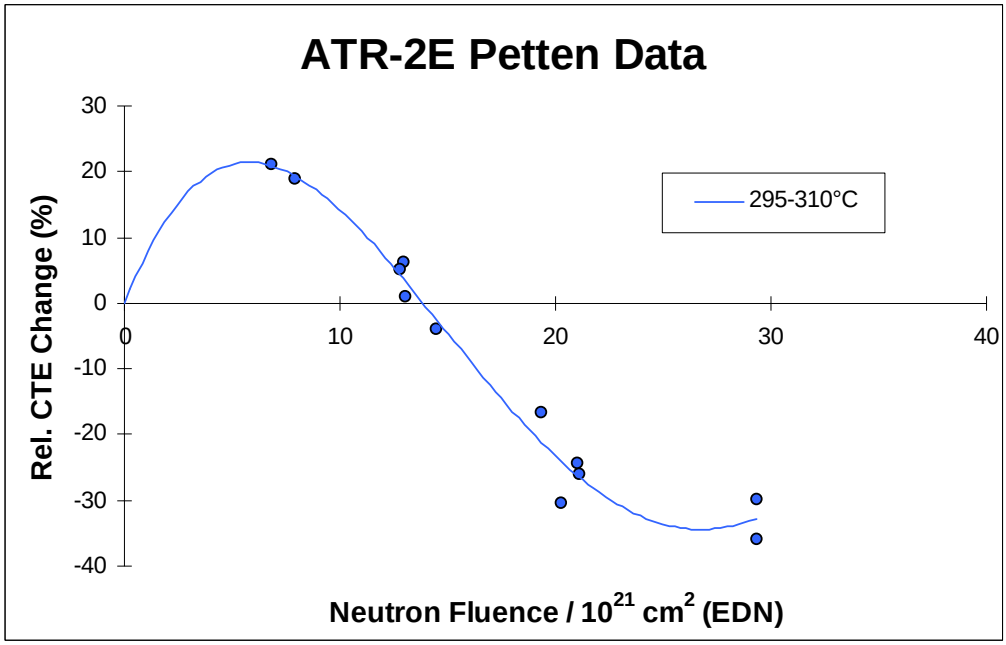

Figure B/3 Relative CTE change (%) - 295-310°C

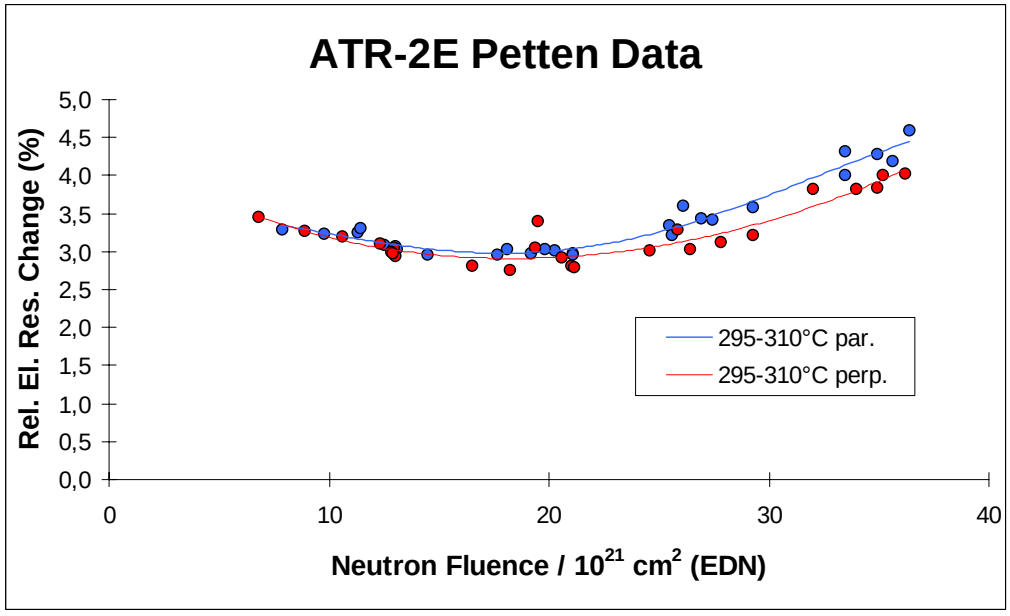

Figure B/4 Relative electrical resistivity change (%) - 295-310°C

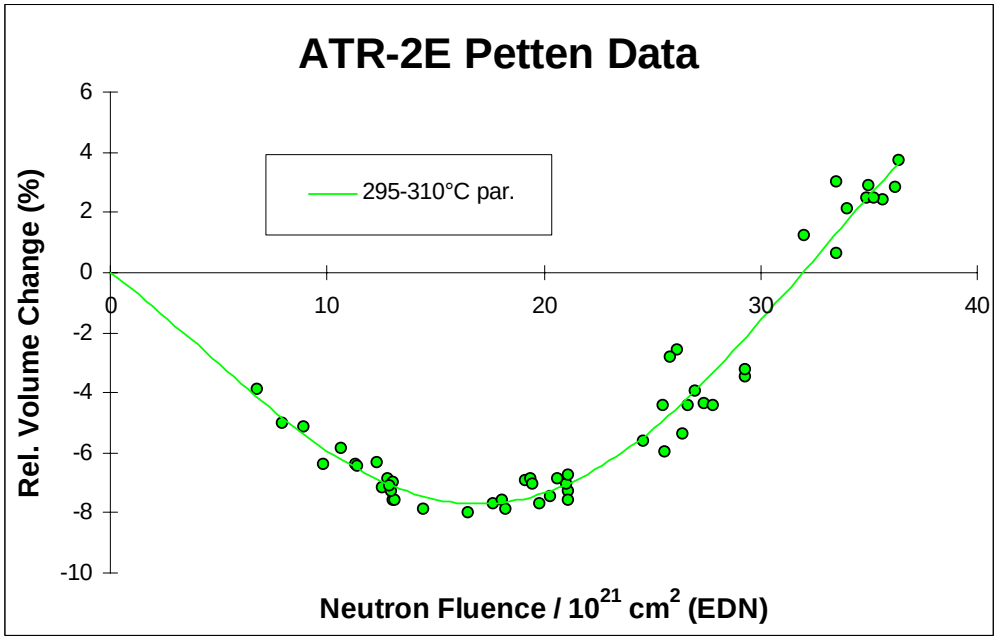

Figure B/5 Relative volume change (%) - 295-310°C

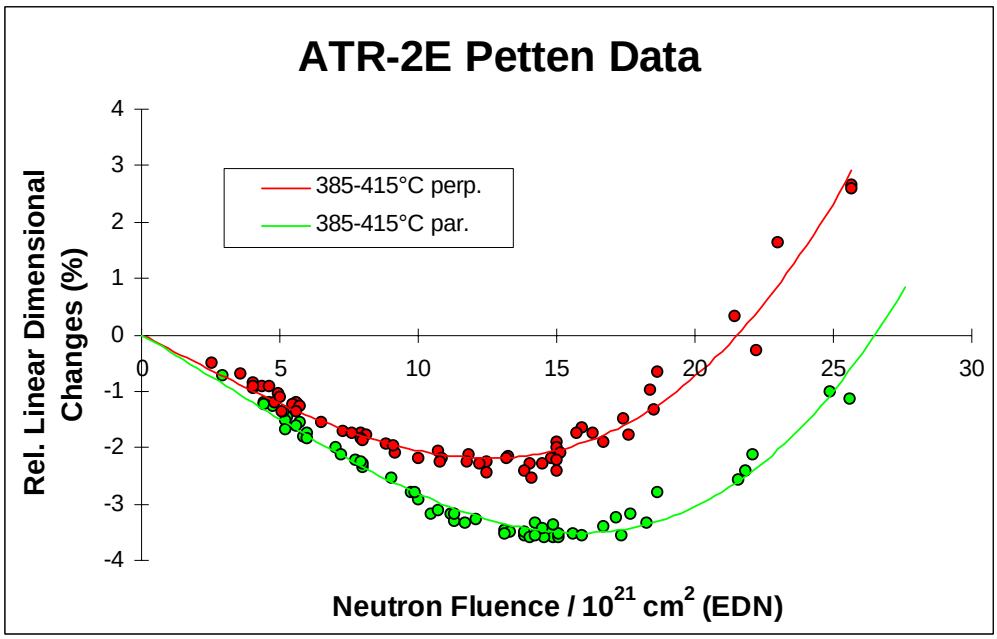

Figure B/6 Relative linear dimensional change (%) - 385-415°C

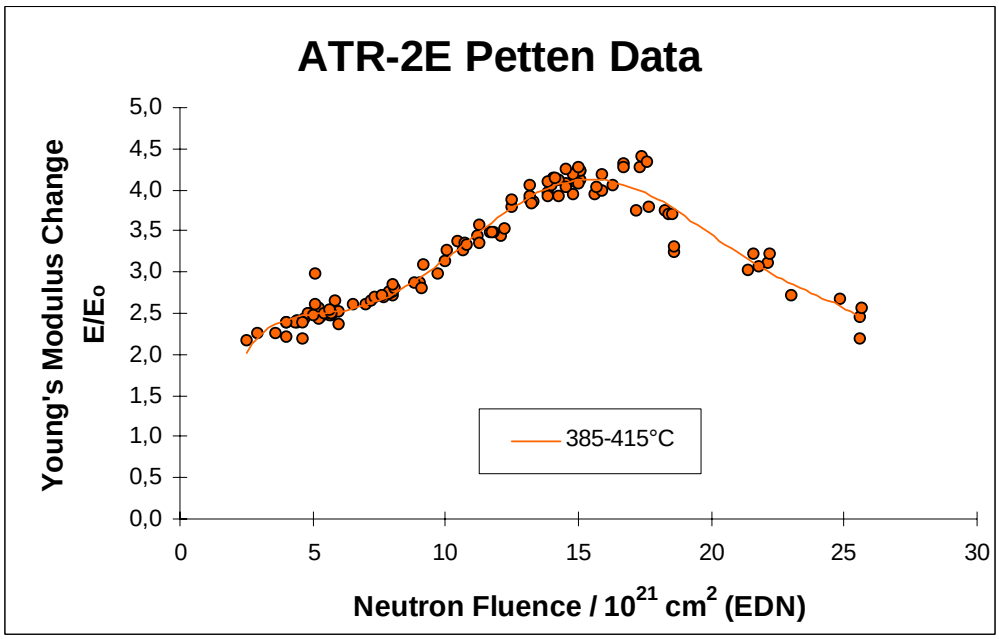

Figure B/7 Relative Young's modulus change (E/Eo) - 385-415°C

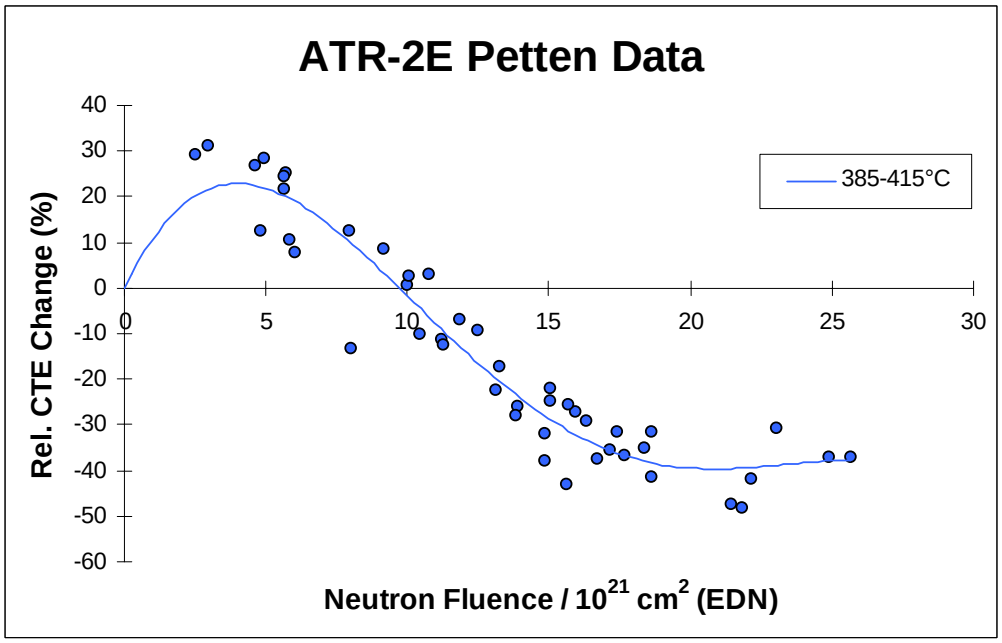

Figure B/8 Relative CTE change (%) - 385-415°C

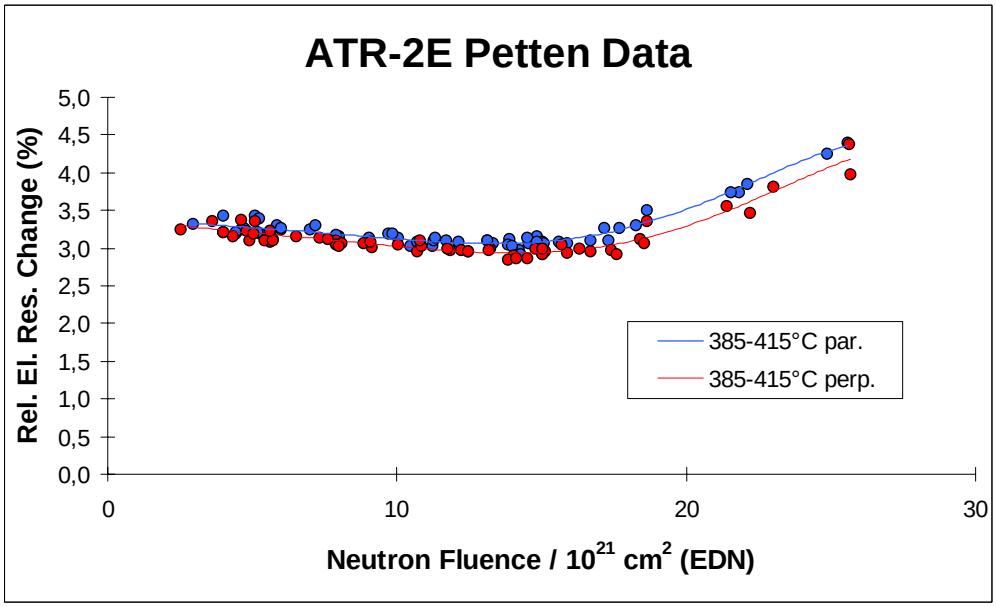

Figure B/9 Relative electrical resistivity change (%) - 385-415°C

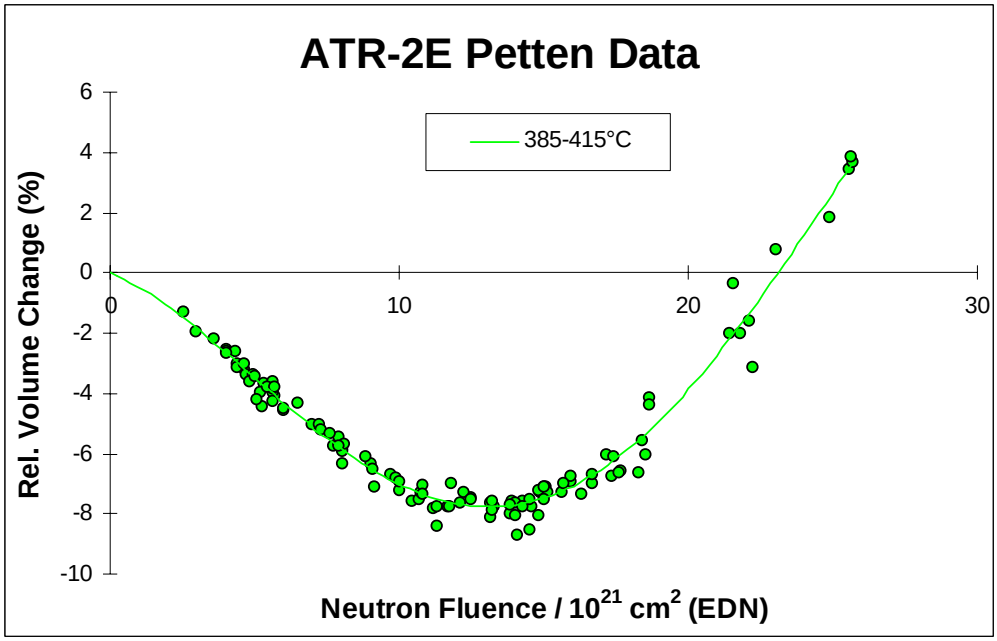

Figure B/10 Relative volume change (%) - 385-415°C

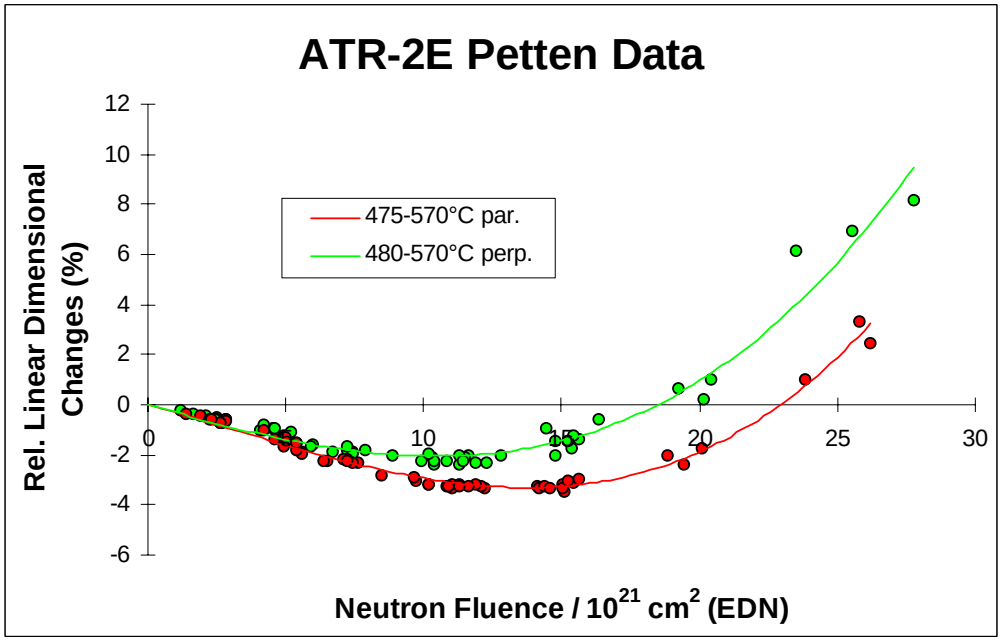

Figure B/11 Relative linear dimensional change (%) - 475-570°C

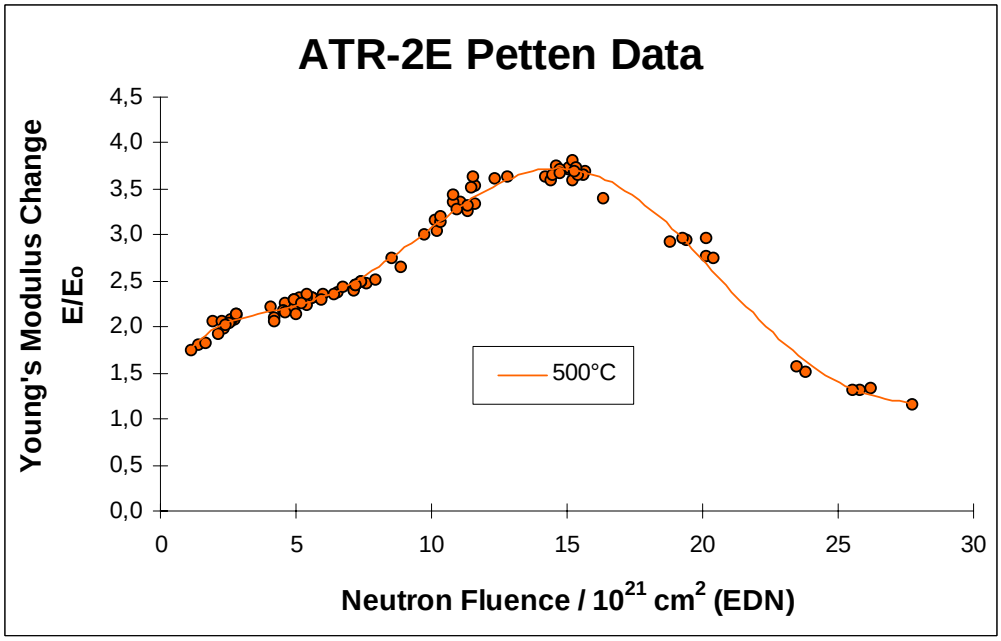

Figure B/12 Relative Young's modulus change (%) - 500°C

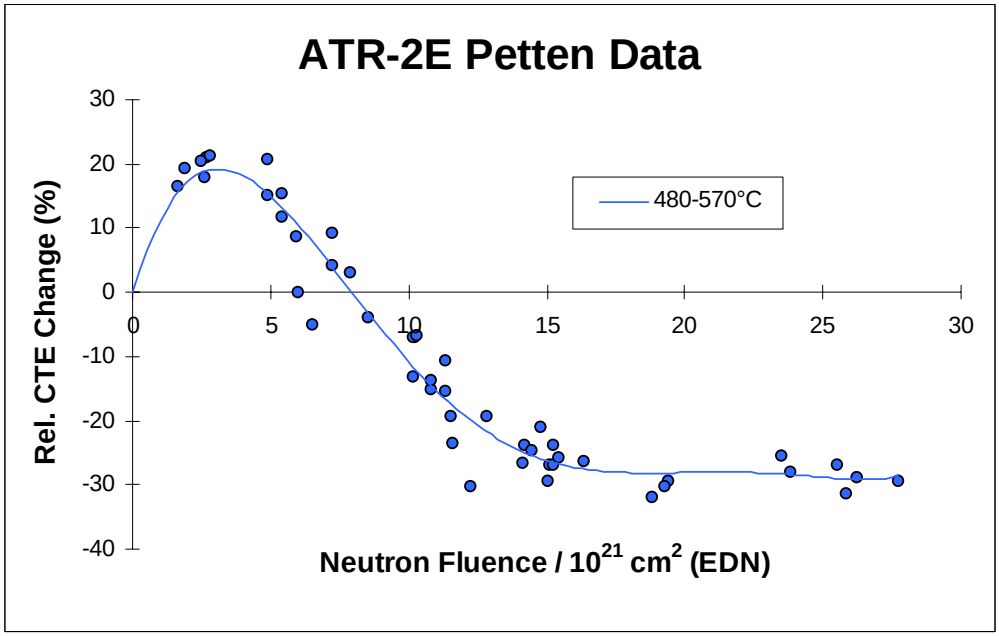

Figure B/13 Relative CTE change (%) - 480-570°C

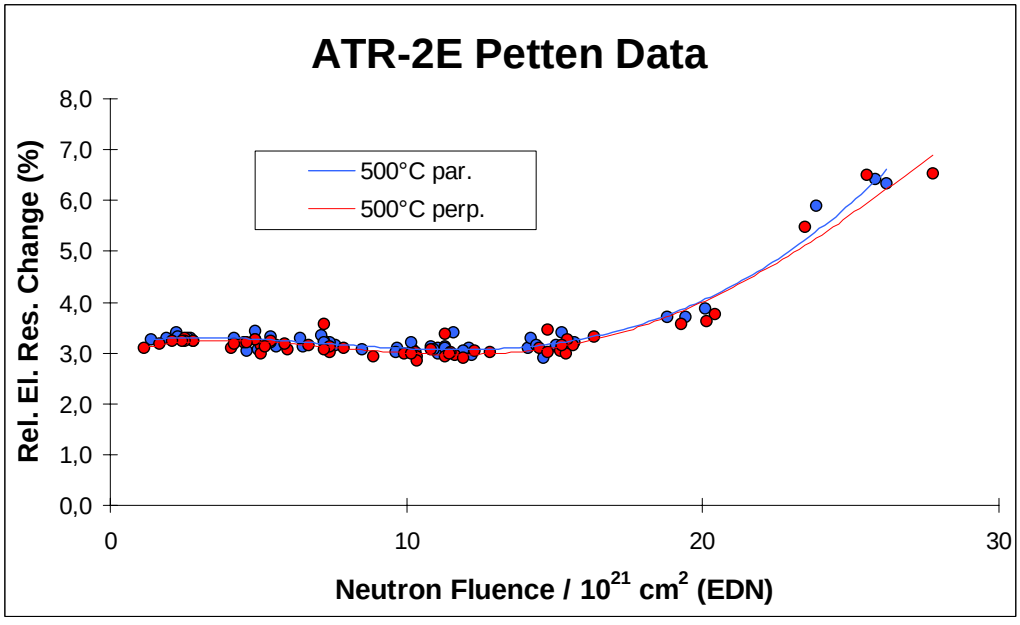

Figure B/14 Relative electrical resistivity change (%) - 500°C

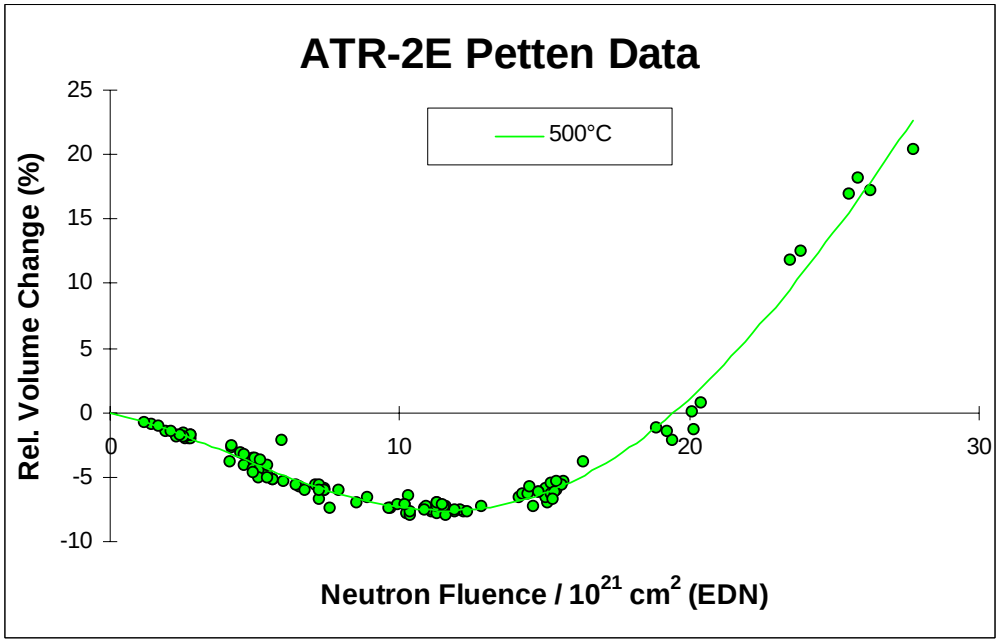

Figure B/15 Relative volume change (%) - 500°C

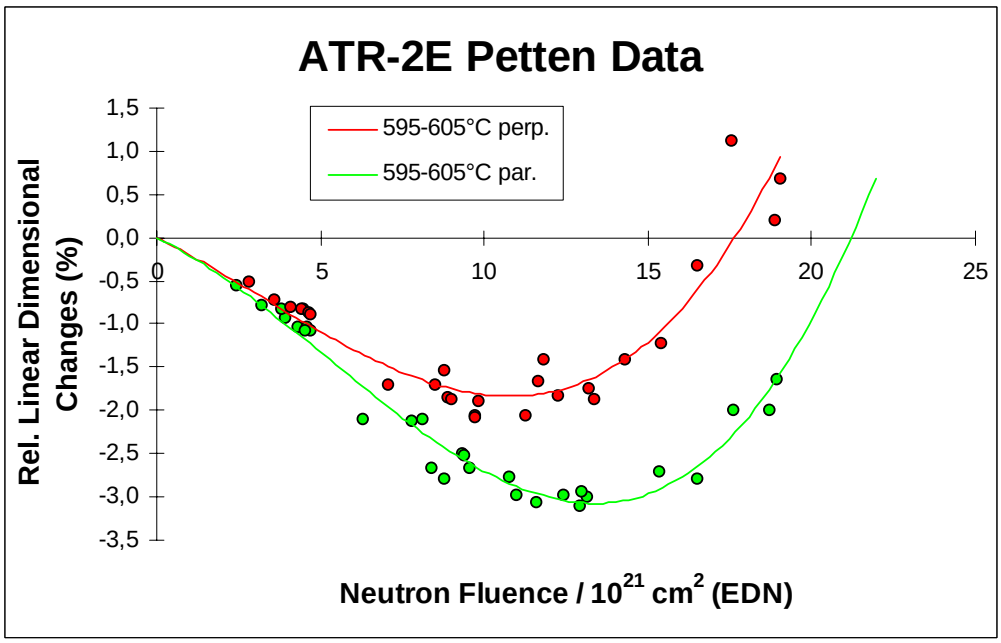

Figure B/16 Relative linear dimensional change (%) - 595-605°C

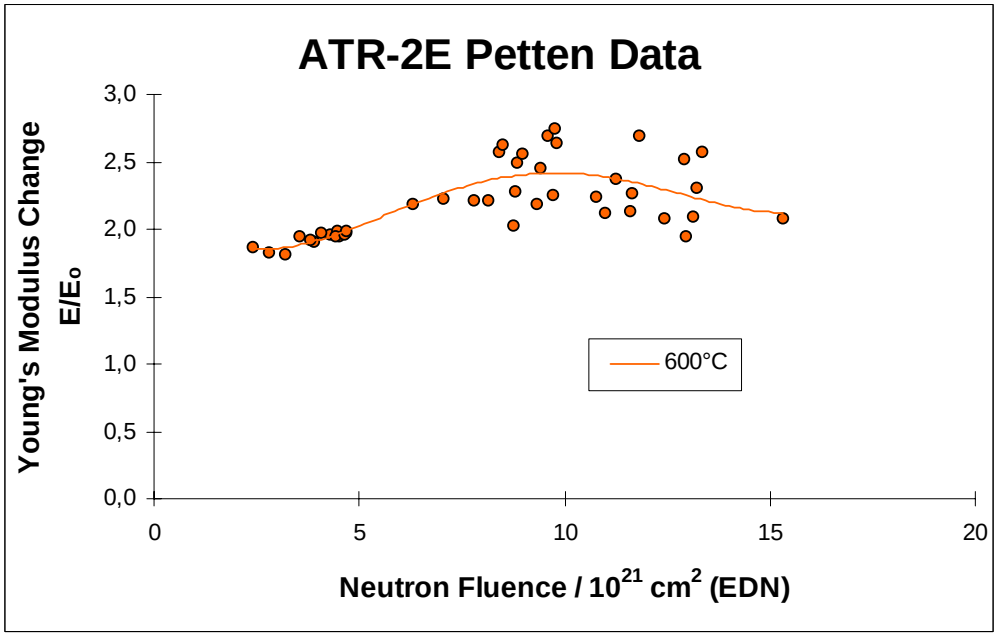

Figure B/17 Relative Young's modulus change (%) - 600°C

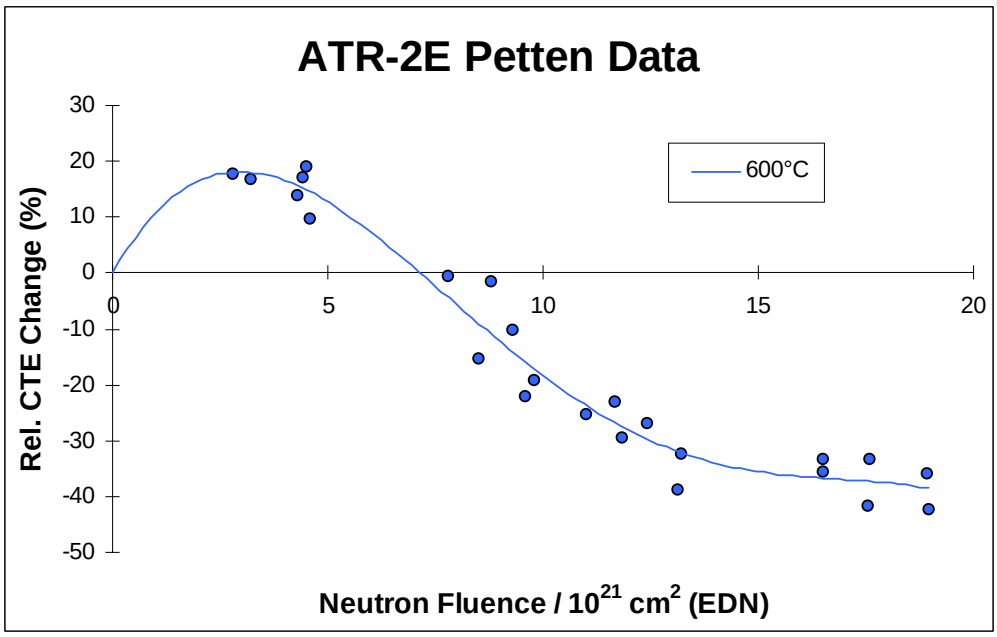

Figure B/18 Relative CTE change (%) - 600°C

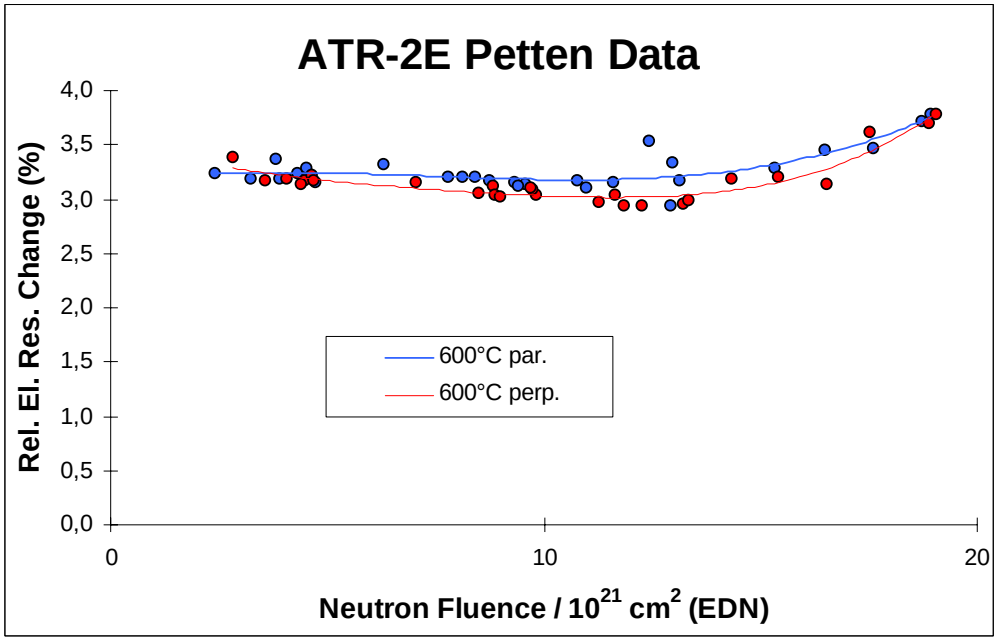

Figure B/19 Relative electrical resistivity change (%) - 600°C

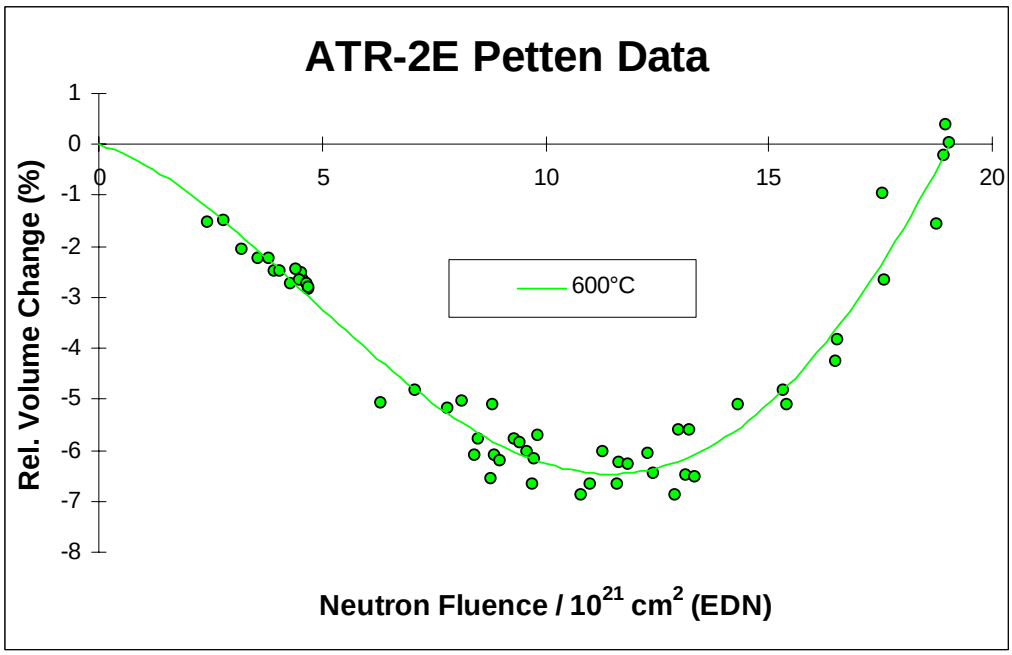

Figure B/20 Relative volume change (%) - 600°C

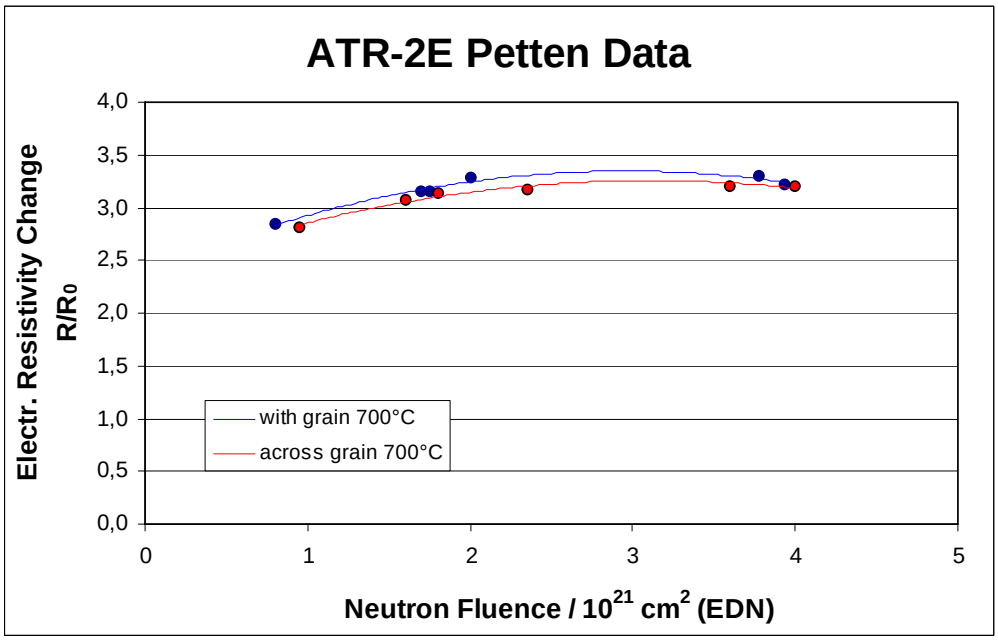

Figure B/21 Relative electrical resistivity change (%) - 700°C

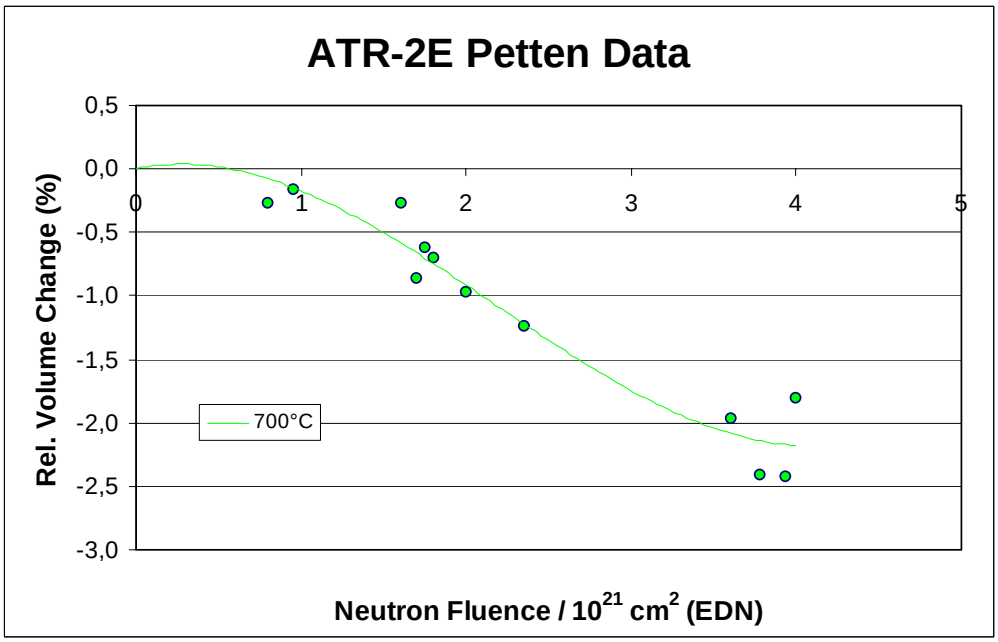

Figure B/22 Relative volume change (%) - 700°C

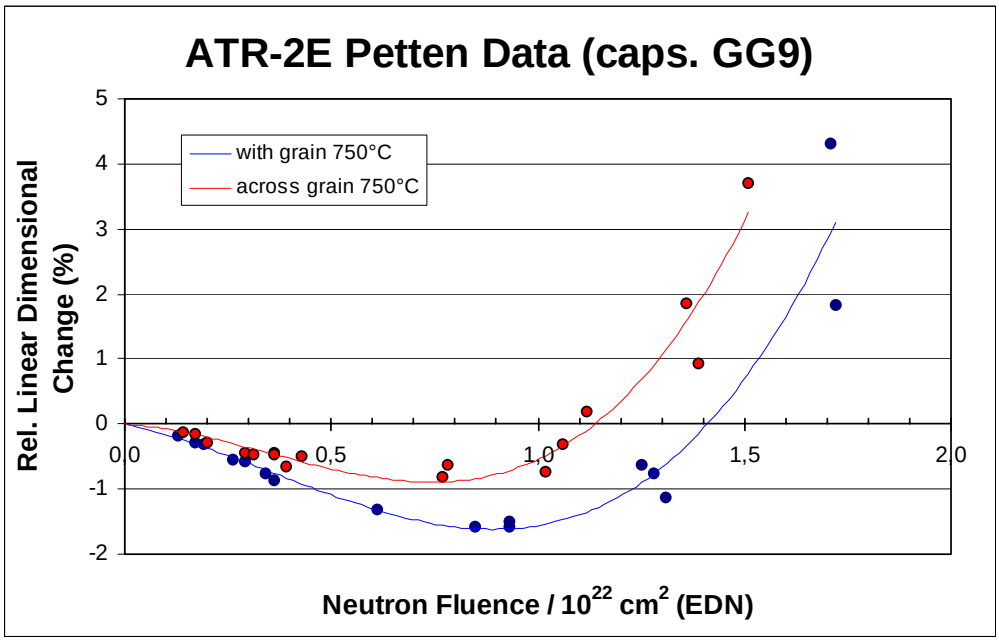

Figure B/23 Relative linear dimensional change (%) - 750°C

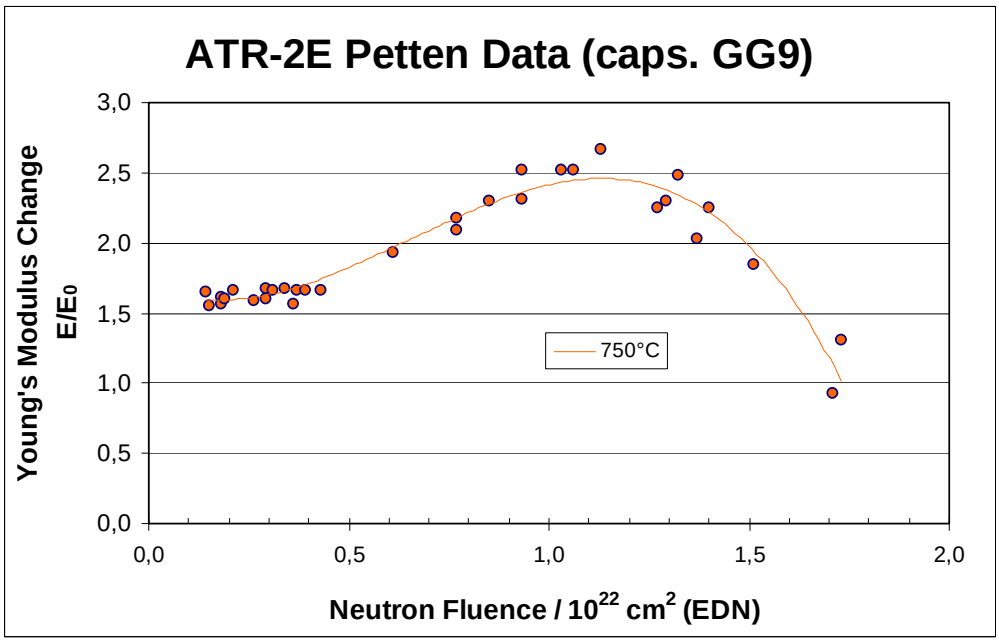

Figure B/24 Relative Young's modulus change (E/Eo) - 750°C

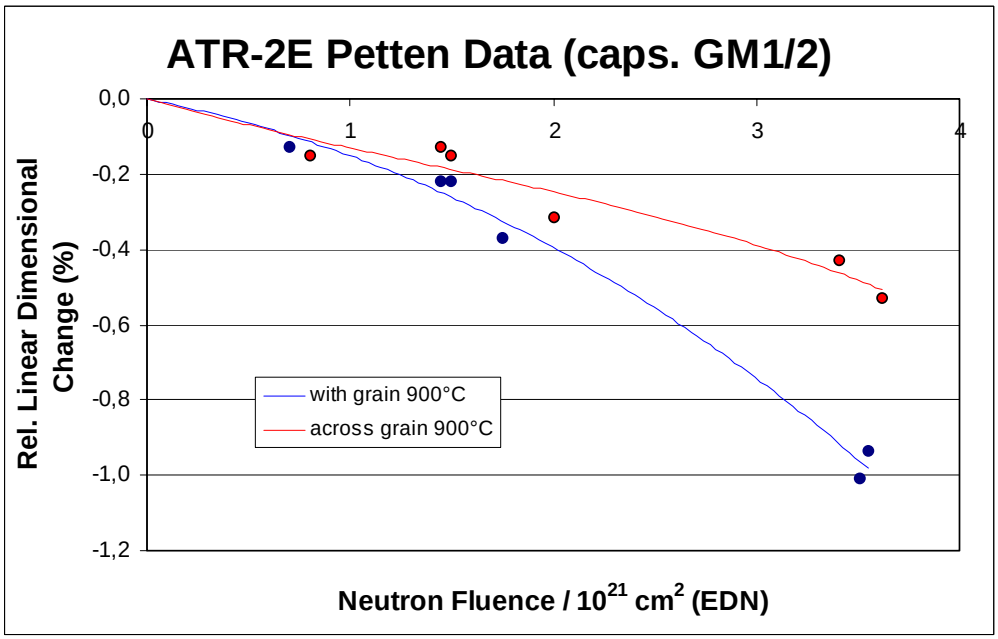

Figure B/25 Relative linear dimensional change (%) - 900°C

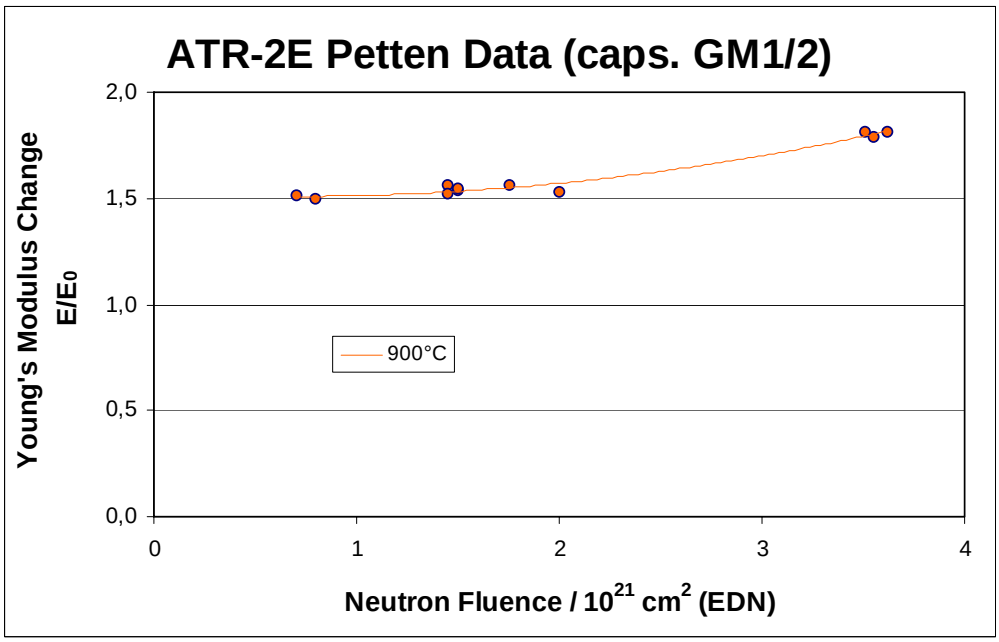

Figure B/26 Relative Young's modulus change (%) - 900°C

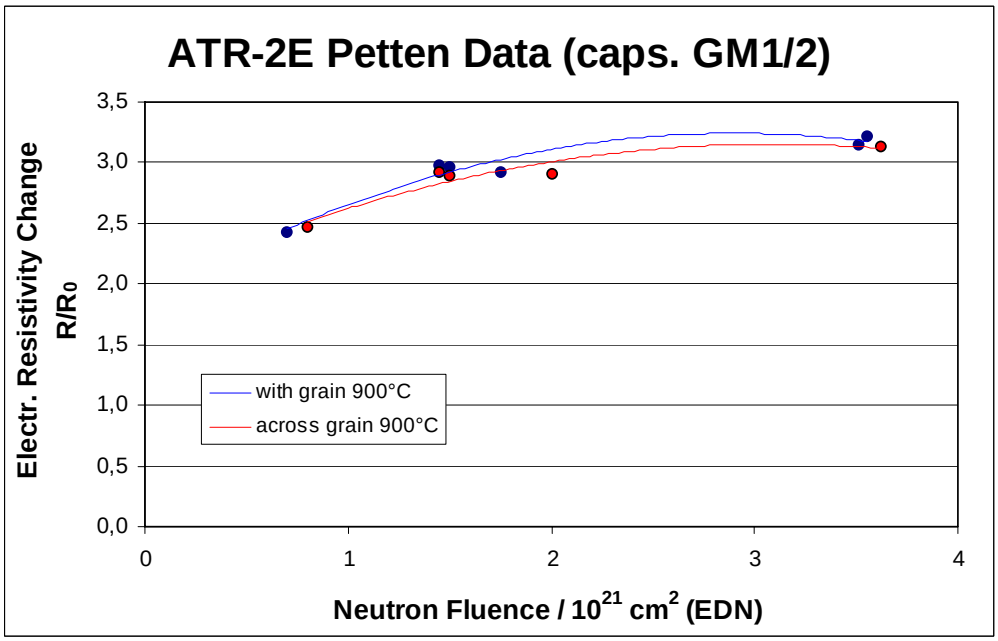

Figure B/27 Relative electrical resistivity change (%) - 900°C

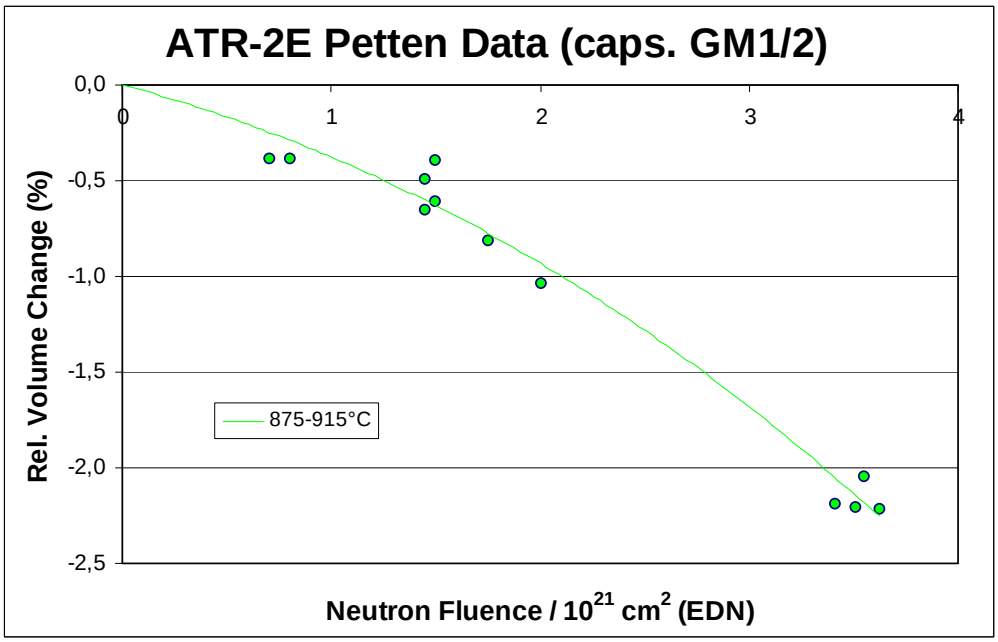

Figure B/28 Relative volume change (%) - 875-915°C

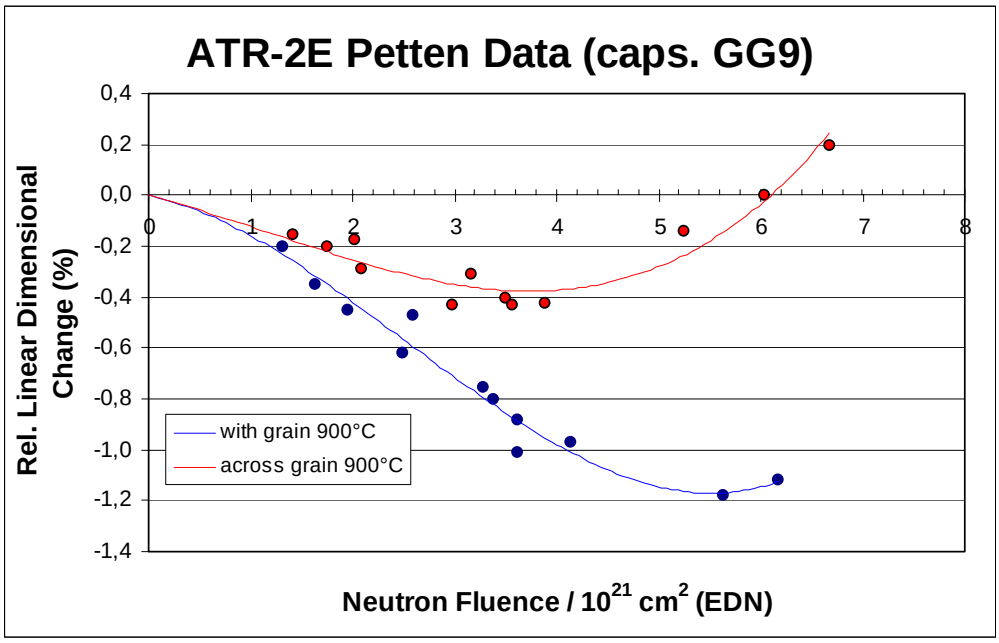

Figure B/29 Relative linear dimensional change (%) - 900°C

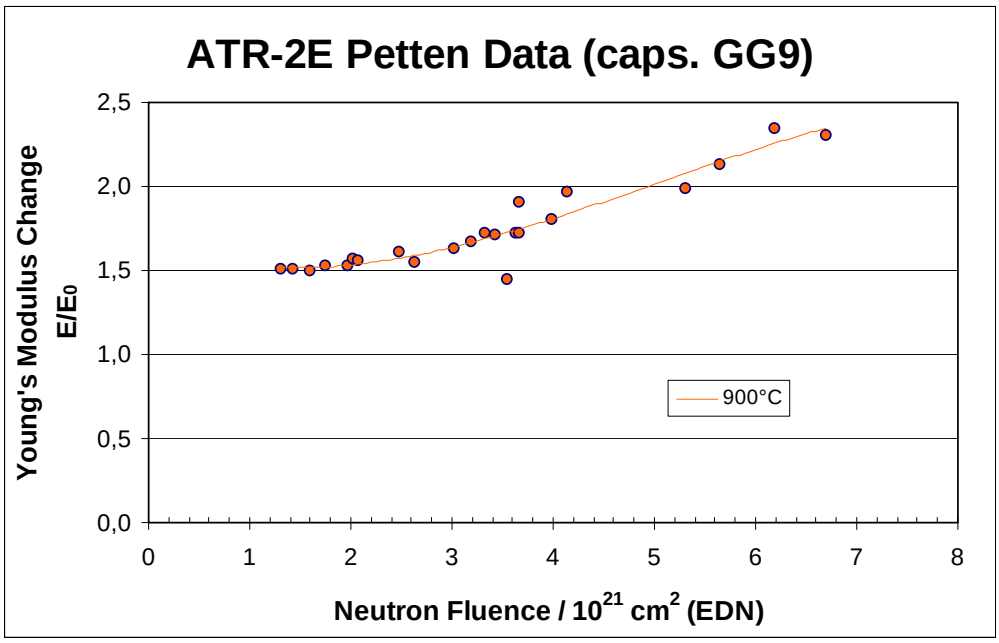

Figure B/30 Relative Young's modulus change (%) - 900°C

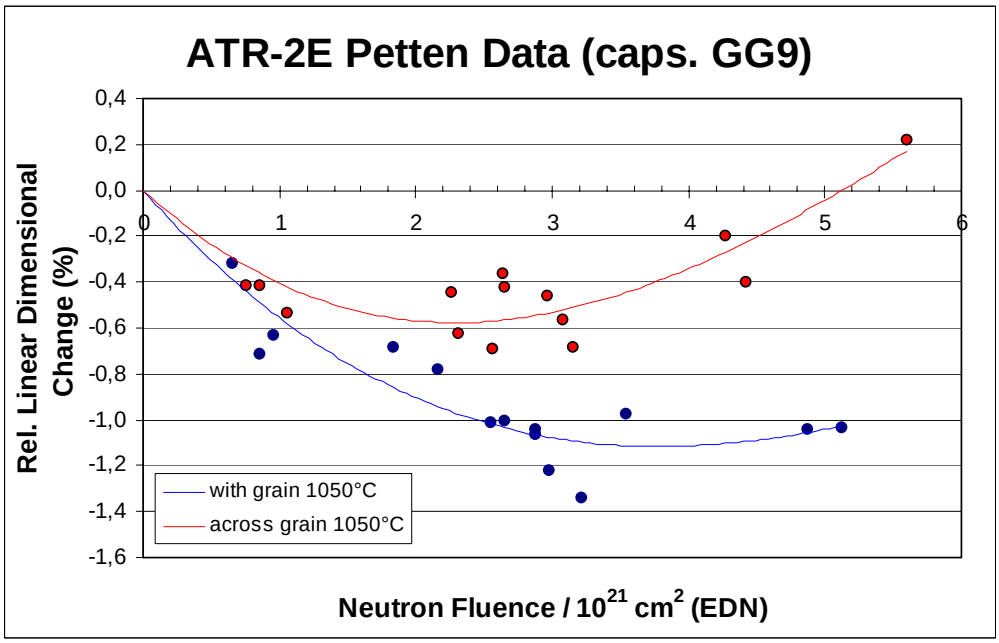

Figure B/31 Relative linear dimensional change (%) - 1050°C

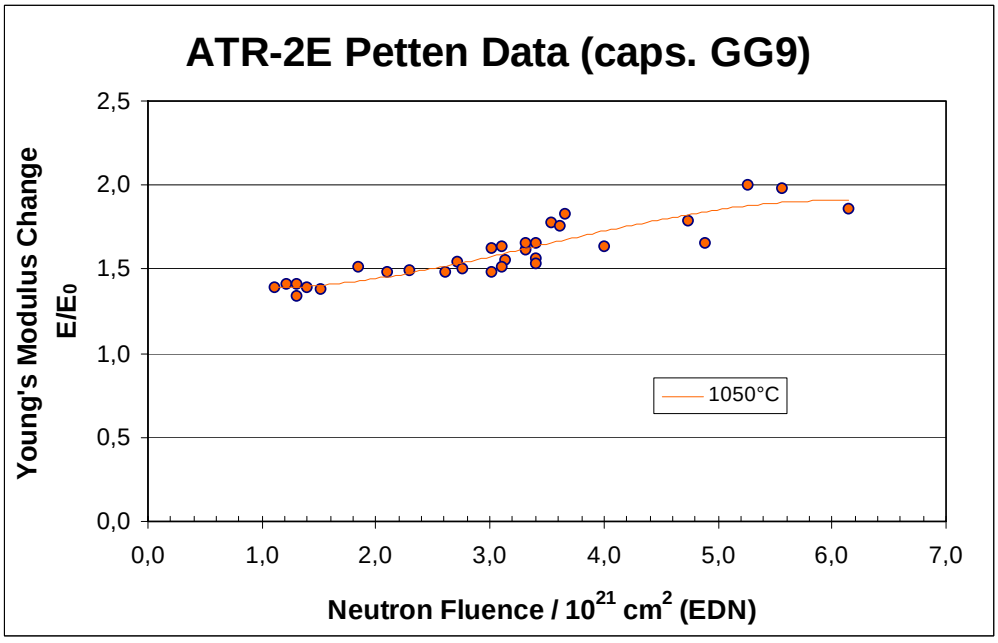

Figure B/32 Relative Young's modulus change (E/Eo) - 1050°C

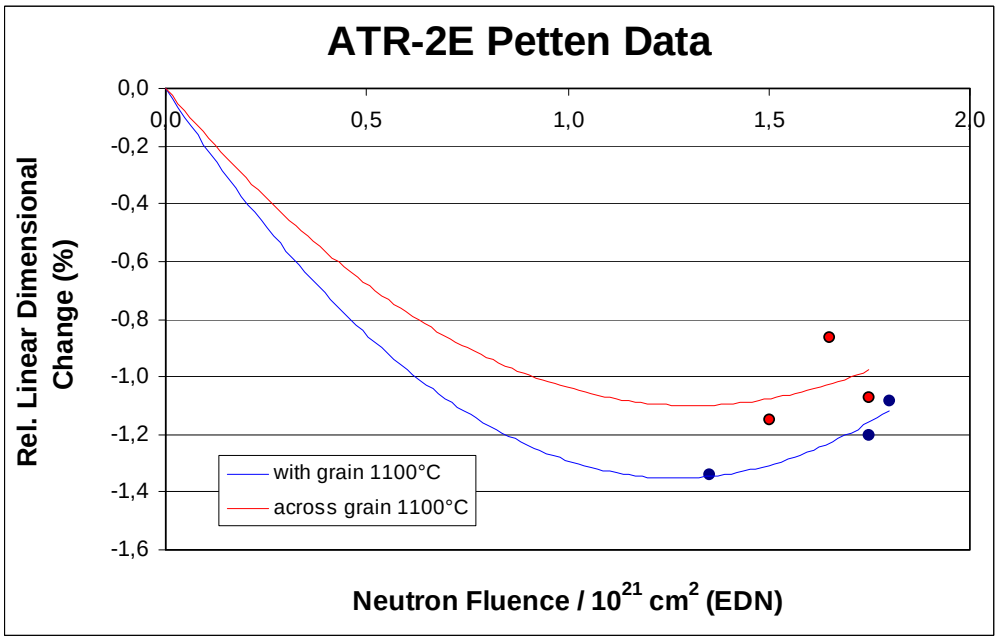

Figure B/33 Relative linear dimensional change (%) - 1100°C

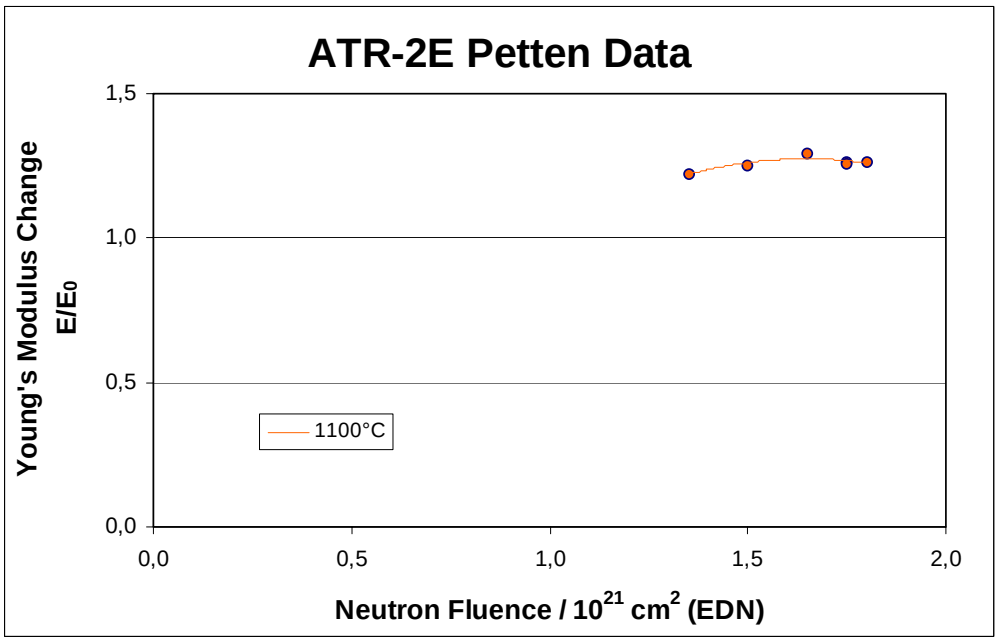

Figure B/34 Relative Young's modulus change (%) - 1100°C

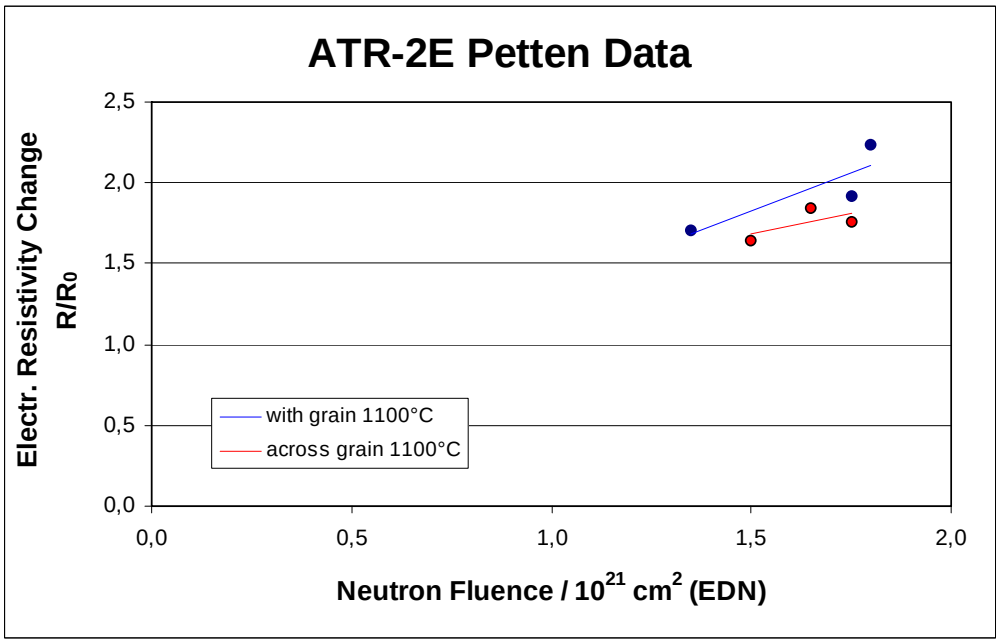

Figure B/35 Relative electrical resistivity change (%) - 1100°C

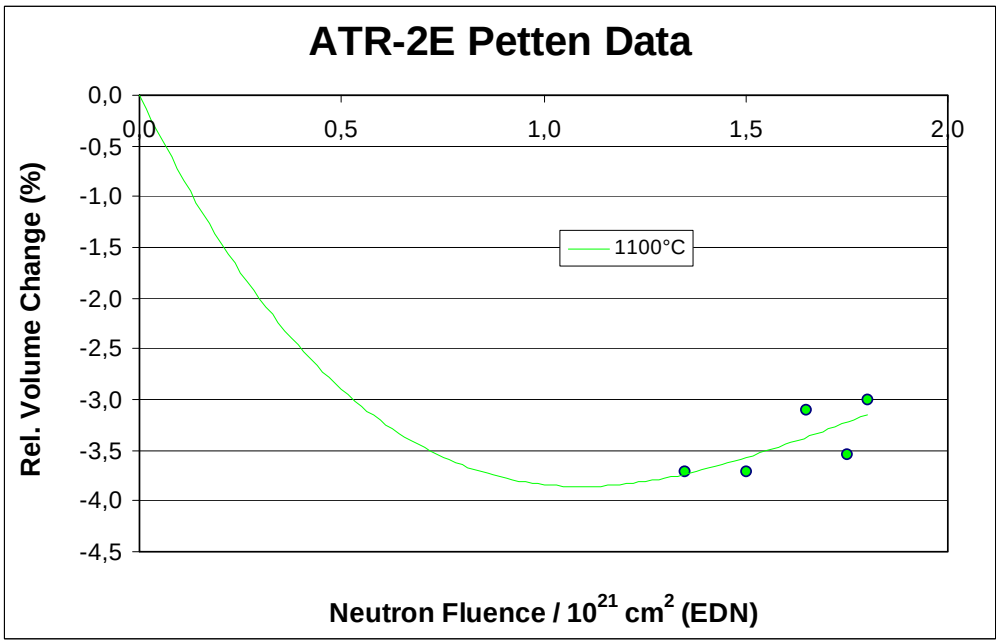

Figure B/36 Relative volume change (%) - 1100°C

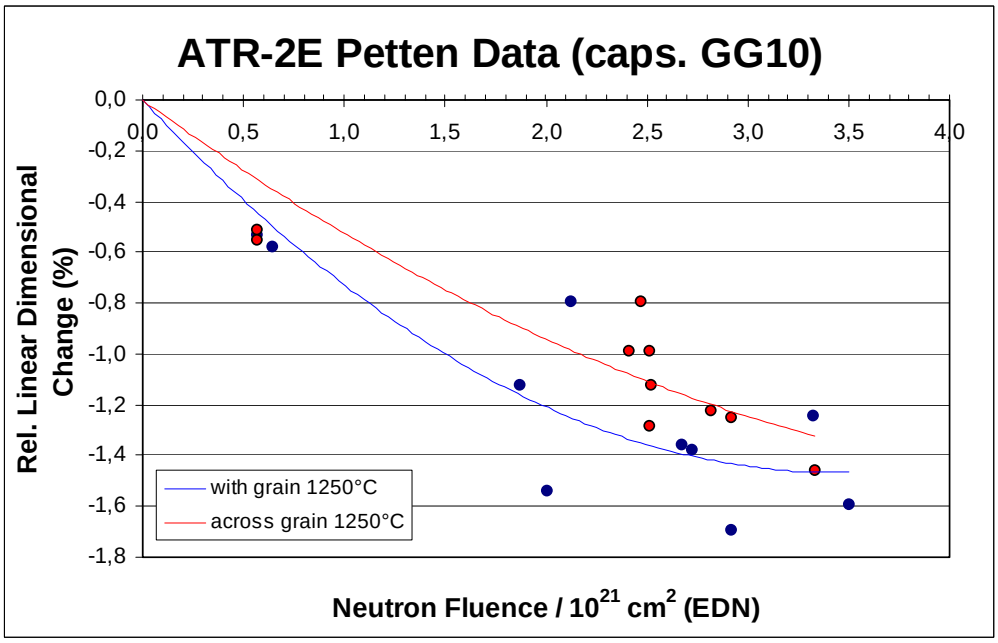

Figure B/37 Relative linear dimensional change (%) - 1250°C

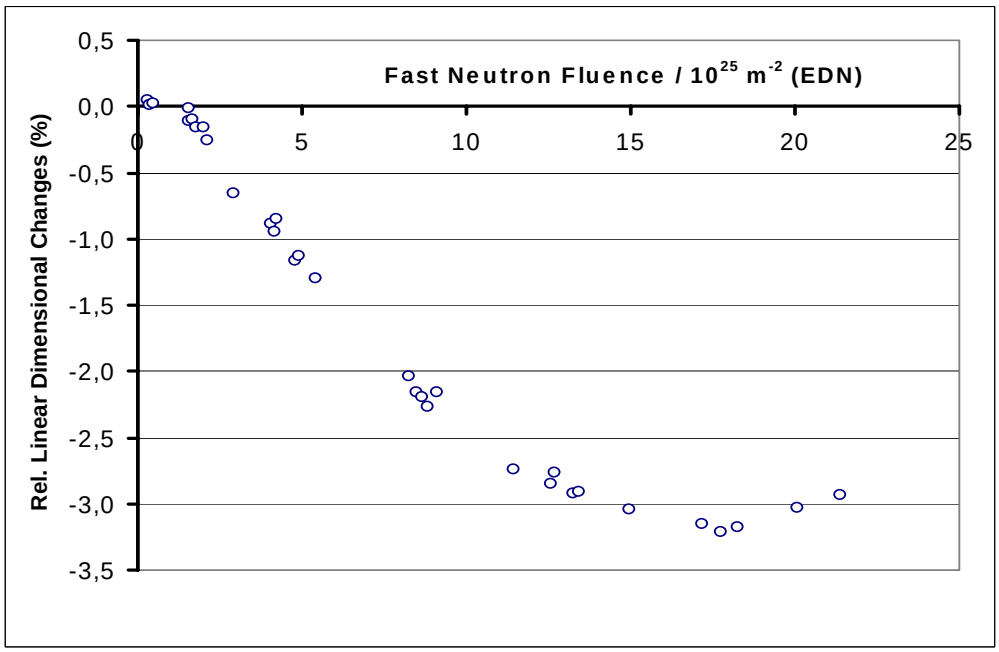

Figure 38 - Dimensional changes of ATR-2E graphite parallel to extrusion direction Irradiation creep at 300°C under tensile load (5 MPa) - Reference specimens (unstressed)

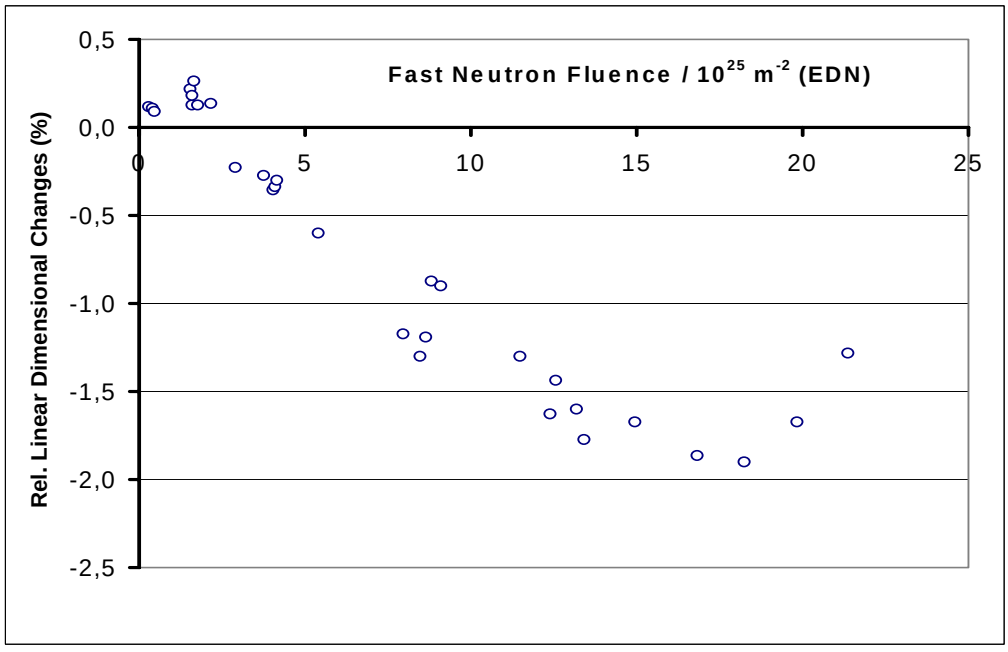

Figure 39 - Dimensional changes of ATR-2E graphite parallel to extrusion direction Irradiation creep at 300°C under tensile load (5 MPa) - Tensile specimens (stressed)

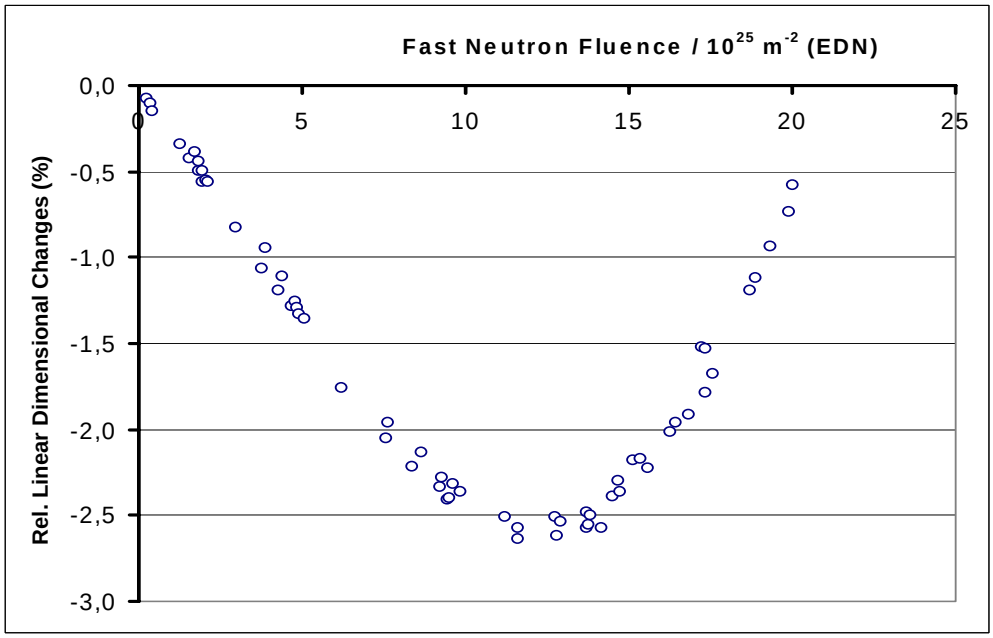

Figure 40 - Dimensional changes of ATR-2E graphite parallel to extrusion direction Irradiation creep at 500°C under compressive load (5 MPa) - Reference specimens (unstressed)

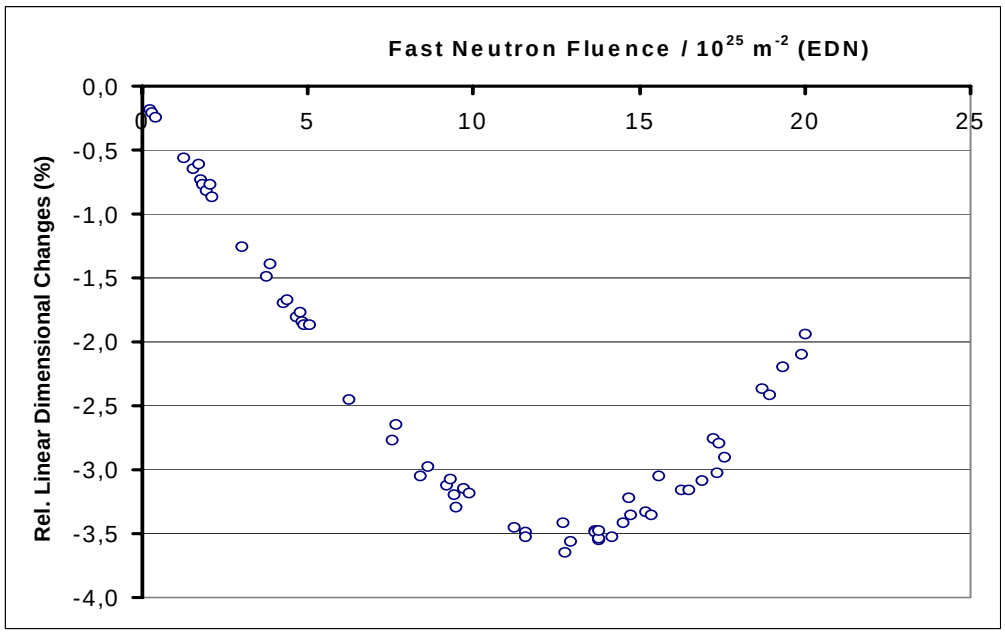

Figure 41 - Dimensional changes of ATR-2E graphite parallel to extrusion direction Irradiation creep at 500°C under compressive load (5 MPa) - Compressive specimens (stressed)

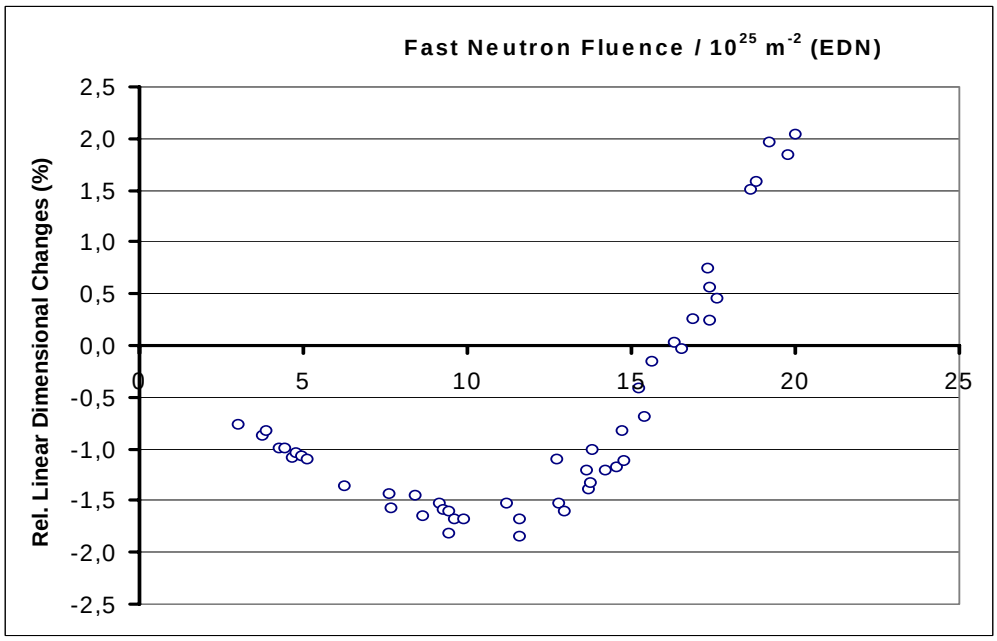

Figure 42 - Dimensional changes of ATR-2E graphite perpendicular to extrusion direction Irradiation creep at 500°C under tensile load (5 MPa) - Reference specimens (unstressed)

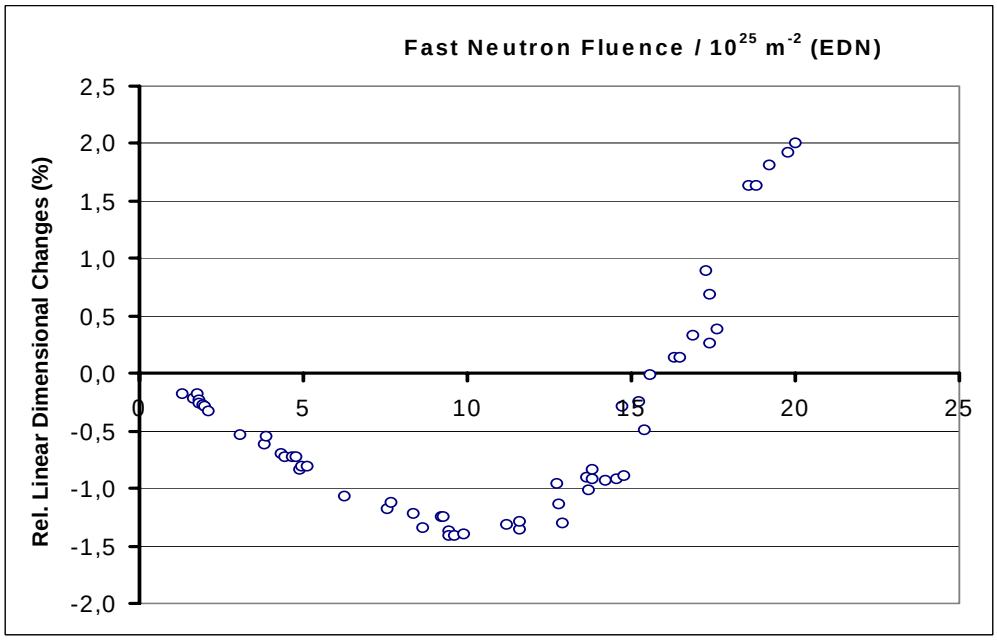

Figure 43 - Dimensional changes of ATR-2E graphite perpendicular to extrusion direction Irradiation creep at 500°C under tensile load (5 MPa) - Tensile specimens (stressed)

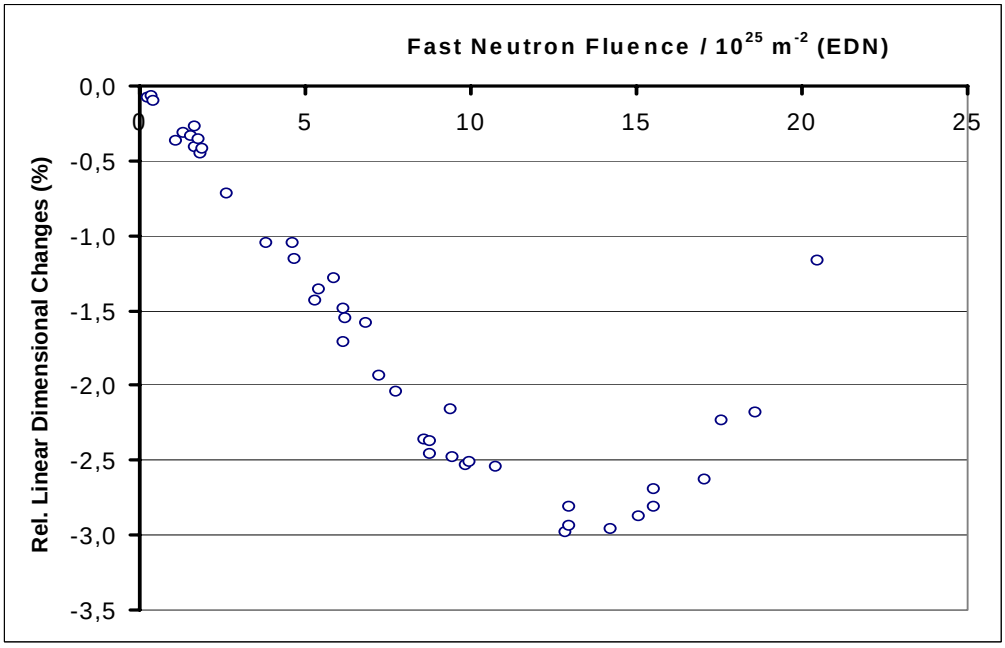

Figure 44 - Dimensional changes of ATR-2E graphite parallel to extrusion direction Irradiation creep at 500°C under tensile load (5 MPa) - Reference specimens (unstressed)

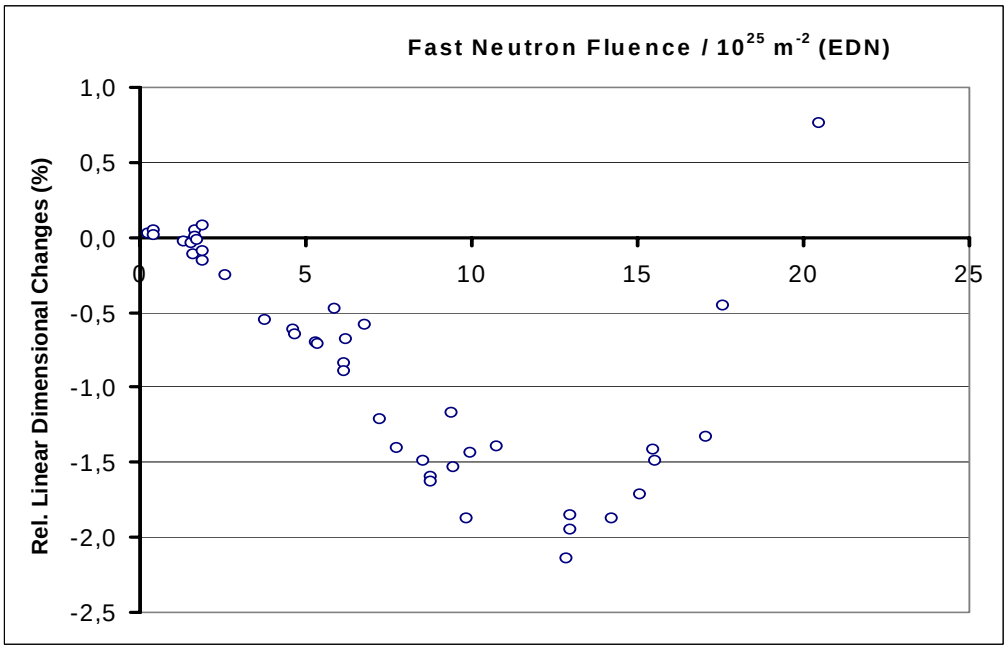

Figure 45 - Dimensional changes of ATR-2E graphite parallel to extrusion direction Irradiation creep at 500°C under tensile load (5 MPa) - Tensile specimens (stressed)